2024

Variation in phenotype and microbiome of three widespread Caribbean corals between mangrove and reef habitats

BOSTON UNIVERSITY

GRADUATE SCHOOL OF ARTS AND SCIENCES

Thesis

VARIATION IN PHENOTYPE AND MICROBIOME OF THREE WIDESPREAD CARIBBEAN CORALS BETWEEN MANGROVE AND REEF HABITATS

by

ZHUOYAN SI

B.S., Pennsylvania State University, 2021

Submit in partial fulfillment of the

requirements of the degree of

Master of Science

2024

Approved by

First Reader _____

John Finnerty, Ph.D.
Professor of Biology

Second Reader _____

Sarah Davies, Ph.D.
Professor of Biology

Third Reader _____

Leslie Kaufman, Ph.D.
Professor of Biology

ACKNOWLEDGEMENTS

I would really like to take this opportunity here to thank all the people who helped me throughout my learning and research journey at Boston University. First of all, I would like to deeply thank Dr. John Finnerty for giving me the chance to learn the beautiful and meaningful coral transplant morphology that could contribute to future coral habitat restoration in marine biology. The ocean and the magical oceanic world has been my love and dream since I was very little, and contributing knowledge and data into conserving the beautiful oceanic world little by little for me felt like a dream come true. I would also like to deeply thank Dr. Karina Scavo Lord for introducing me to her ambitious big research ideas on coral restoration and sharing her coral samples collected from Belize with me to help me with my research projects generously. I would also like to sincerely thank Joanna Lee and Karina for teaching me patiently about R studio and coding for data analysis methods.

For my research thesis acknowledgements, I would like to state that the coral samples in chapter 1 and chapter 2 were collected by Karina Scavo Lord. The research ideas from chapter 1 were from John Finnery and Karina Scavo Lord, and the research ideas from chapter 2 were from John Finnerty, Karina Scavo Lord, and Hannah Aichelman. All the 16S sequencing process was done by

students from John Finnerty's marine genomics class in 2021. In chapter 2, the research on two Caribbean corals (*Porites astreoides* and *Siderastrea siderea*) microbiome varieties between mangrove and reef habitats was a collaborative project, and my roles were to analyze microbiome diversity between two coral species across two habitats using chloroplasts genomes and to identify indicator species with archaea and chloroplast genomes from coral samples.

VARIATION IN PHENOTYPE AND MICROBIOME OF THREE WIDESPREAD CARIBBEAN CORALS BETWEEN MANGROVE AND REEF HABITATS

ZHUOYAN SI

ABSTRACT

Coral reef ecosystems are increasingly threatened by anthropogenic forces, especially climate change. However, many reef corals also occur in mangrove habitats. For example, in the Caribbean, roughly half of the ~75 coral species found on reefs also inhabit mangroves. The ability to inhabit both reefs and mangroves may promote the survival of these generalist corals, but environmental conditions are quite different on reefs and mangroves, challenging corals to adopt different phenotypes and perhaps assemble distinctive microbiomes in order to survive in different habitats. In Belize's Turneffe Atoll Marine Reserve, mangrove corals have been found to experience significantly lower light levels, higher peak temperatures, and greater temperature variability than conspecifics living in lagoonal patch reefs. Significant differences in colony morphology, color and

corallite dimensions were also found across habitats. To understand whether the differences in phenotype of the same coral species from both habitats were plastic or fixed, fragments of the club finger coral, *Porites porites,* were subjected to reciprocal transplantation between reef and mangrove habitats. Corallite morphological differences on the transplant samples between two habitats were examined, measuring corallite area, spacing, and density. Regardless of their native habitat (reef or mangrove), corals transplanted to the reef exhibited greater corallite density, smaller corallite area, and reduced corallite spacing. When transplanted to the same habitat, mangrove-sourced corals exhibited greater corallite density, as well as smaller corallite area, and reduced corallite spacing. To understand how the microbiome varies in corals living across habitats, metagenomic approaches were used to compare the bacterial, archaeal, and eukaryotic photosynthetic components of the holobiont in two widespread corals — *Porites astreoides* and *Siderastrea siderea* — across mangrove and lagoon habitats. Indicator species analyses revealed many significant bacteria, archaea, and photosynthetic eukaryotes that differed significantly among the four species-by-habitat combinations. Understanding what corallite morphological traits and microbiome components of the corals surviving in mangrove habitats could offer insight into promoting these traits and components and increasing chances of survival in harsh environments for corals in peril.

TABLE OF CONTENTS

LIST OF FIGURES

CHAPTER ONE

CHAPTER TWO

LIST OF ABBREVIATIONS

ANOVA	Analysis of Variance
ASV	Amplicon Sequence Variant
NMDS	Non-metric Multidimensional Scaling
NT	Nucleotides
OTU	Operational Taxomonic Unit
PERMANOVA	Permutational Multivariate Analysis of Variance

CHAPTER ONE

VARIATION IN CORALLITE MORPHOLOGY (AREA, SPACING, AND DENSITY) OF CARIBBEAN CORAL *PORITES PORITES* TRANSPLANTS BETWEEN MANGROVE AND REEF HABITATS

Introduction

Coral reef ecosystems are increasingly threatened by anthropogenic environmental change, especially climate change (Hughes et al. 2003; Hoegh-Guldberg et al. 2007; Munday et al. 2013), however, many "reef corals" can also be found in mangrove habitats, where the environmental conditions are quite different from those on the reef. For example, in the Caribbean, approximately half of the ~75 species of coral dwelling on reefs can also be found in mangroves (Rogers and Herlan 2012; Hernández Fernández 2015; Bengtsson et al. 2019). Mangrove habitats have lower light levels and higher and more variable temperatures than reef habitats (Camp et al. 2016; Scavo Lord et al. 2021). Studies have shown that corals exposed to greater temperature variability can exhibit higher thermally induced bleaching resistance (Scavo Lord et al. 2020; Castillo and Helmuth 2003; Oliver and Palumbi 2011; Palumbi et al. 2014). Therefore, mangroves may be selected for corals with greater tolerance to thermally-induced bleaching (Camp et al. 2016). Alternatively, mangroves may represent an ecological refuge because shading from the canopy reduces the amount of UV radiation to which the corals are exposed (Yates et al. 2014). Whether mangroves provide a reservoir of thermally resilient individuals (Camp et al. 2016), or they provide an ecological refuge (Yates et al., 2014), they may be playing a critical role in the survival of those generalist corals that can inhabit both reef and mangrove habitats.

However, while the ability to occupy mangrove habitats may increase coral resilience, the distinct environmental conditions may also require corals to adopt distinct phenotypes in order to survive. A previous study at Turneffe Atoll, Belize demonstrated that corals of the same species —thin finger coral (*Porites divaricata*) and Mustard Hill Coral (*P. astreoides*)— living in a shallow sunny lagoon or living as epibionts on the prop roots of red mangrove (*Rhizophora mangle*) differed in key phenotypic traits including colony form, colony color, and micro skeletal architecture (Scavo Lord et al., 2021). Specifically, corals living in the lagoon had higher ecological volume, lower red color density, and smaller branch number compared to mangrove corals. As this study compared naturally occurring lagoon and mangrove colonies, it could not determine whether differences in phenotype were driven by local adaptation or phenotypic plasticity, or a combination of the two. In order to differentiate between local adaptation and phenotypic plasticity, reciprocal transplants were performed on another poritidae coral that is found in Belize reefs and mangroves, the Club Finger Coral, *Porites porites* (Scavo Lord, in prep). As part of this study, I measured key corallite dimensions—corallite area, corallite density, and corallite spacing — to determine how transplantation impacted skeletal phenotype, and whether corals sourced from different habitats would converge on skeletal phenotypes when transplanted to the same habitat, reef or mangrove.

If corallite phenotypic characteristics are environmentally plastic, then the corallite traits (area, spacing, density) should be dependent on habitat regardless of where the transplants were sourced. However, if the corallite phenotype differences are fixed, due to either genetic differences or epigenetic mechanisms, then the corallite traits (area, spacing, density) should be consistent between transplants sourced from the same habitat, regardless of the habitat to which they are transplanted.

Materials and methods

Focal coral species

Club Finger Coral, *Porites porites* (Figure 1.1a, b), is a branching coral common to reef habitats throughout the Caribbean, where it can be found at depths of 0.5 m to 35 m (Veron 2000). More recently, *P. porites* has also been found to be a common member of mangrove coral communities (Rogers and Herlan 2012; Hernández Fernández 2015; Rogers 2017; Bengtsson et al. 2019) (Figure 1.2a, b).

Figure 1.1. *Porites porites* in lagoon patch-reef habitat. **A.** *P. porites* [Pp] colony in association with *P. astreoides* [Pa], *Siderastrea siderea* [Ss], and *Thalassium testudinum* [Tt]. **B.** Close up of extended polyps from the colony shown in **A.** Photos were taken by J. R. Finnerty in Long Bogue, Turneffe Atoll, Belize.

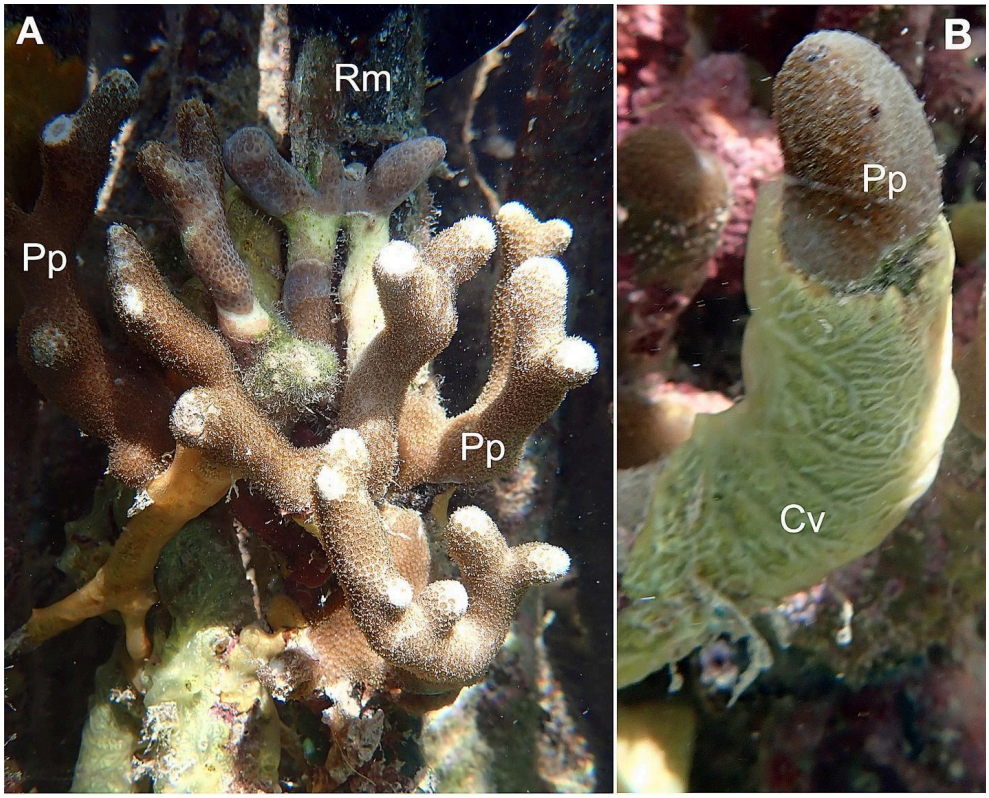

Figure 1.2. *Porites porites* growing upon a prop root of the Red Mangrove (*Rhizophora mangle*; [Rm]). **A.** A *P. porites* [Pp] colony experiences uneven lighting due to shading from the mangrove canopy. **B.** Close up of a single branch of *P. porites* [Pp] that is extensively overgrown by a sponge, likely *Clathria venosa*, a mangrove endemic species [Cv]. **A.** Photos were taken by J. R. Finnerty at Calabash Caye, Belize.

Establishment of Coral Transplants

In November of 2017, three colonies (1,2,3) of *P. porites* from a mangrove habitat and three colonies (4,5,6) of *P. porites* from a reef habitat were chosen from nearby shallow-water locations on Turneffe Atoll, Belize (Fig 1.3). The mangrove colonies used to source transplant material were growing as epibionts

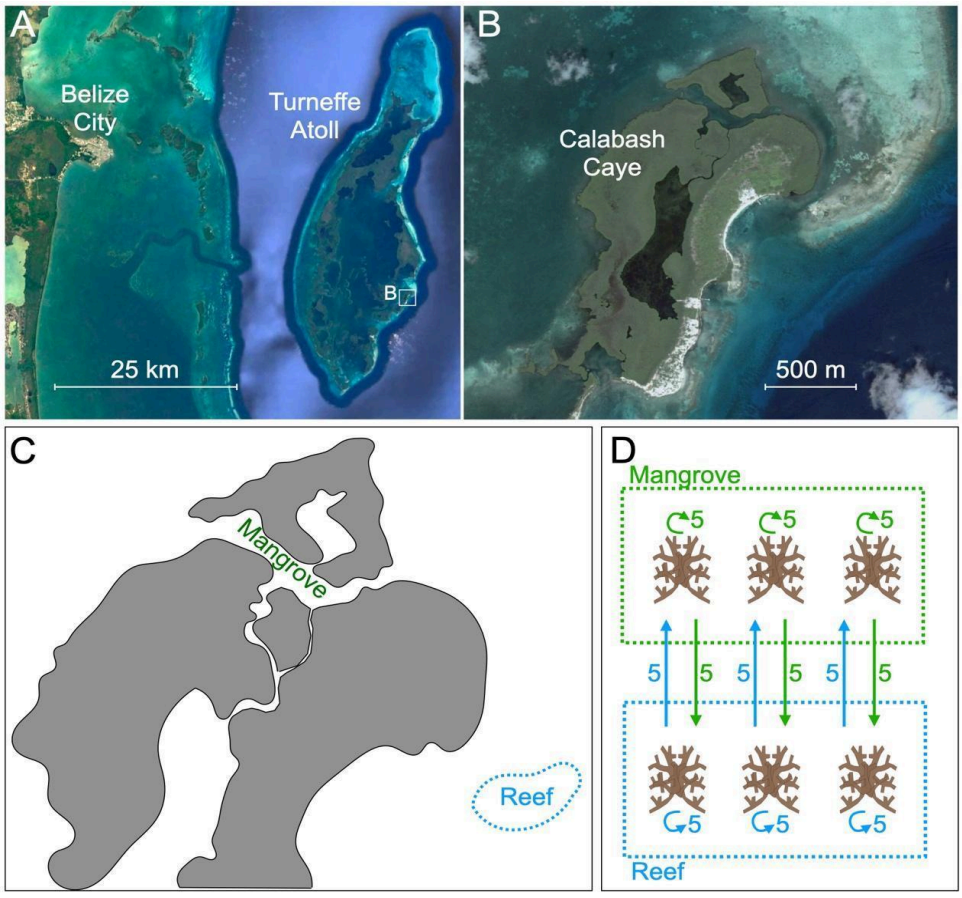

Figure 1.3. Study site and transplant study design. **A.** Turneffe Atoll. The location of Calabash Caye is indicated by the square (B). **B.** Calabash Caye. **C.** Diagram of Calabash Caye with location of mangrove and reef colonies used in transplant indicated. D. Scheme for transplanting ten branch tips from each of six corals, three from the mangrove and three from the reef. For each coral, five branch tips

were transplanted within the native habitat and five were transplanted to the alternative habitat.The satellite photos of Turneffe Atoll and Calabash Caye were accessed via Google Earth Pro, v. 7.3.6.9796, 2024, Maxar Technologies.

upon the prop roots of red mangrove (*Rhizophora mangle*). Ten branch tips, roughly 3 cm in length, were taken from each coral colony. Five branch tips per colony were transplanted back into the source habitat (reef-to-reef or mangrove-to-mangrove) and five were transplanted into the alternative habitat (reef-to-mangrove or mangrove-to-reef). All branch tips transplanted into the reef habitat were secured to round PVC disks known as "cookies" using marine epoxy. The cookies were then affixed to hard substrates in the reef using marine epoxy (IC-Gel Insta Cure Cyanoacrylate Coral Frag Glue; Bob Smith Industries). All branch tips transplanted into the mangrove were epoxied to custom PVC platforms that were then zip-tied to mangrove prop roots. The platforms were constructed as follows. First, a section of 2.5-inch PVC pipe roughly 20 cm in length was cut in half longitudinally (Fig 1.4a,b). Then, approximately 8 cm from the bottom of the sectioned pipe, two transverse notches were cut into the pipe from the center towards the perimeter, leaving a thin tab connecting the upper and lower sections (Fig 1.4c). This thin tab was then heated with a heat gun until the bottom section of the pipe could be bent outward, creating a small platform where the coral transplant could be epoxied (Fig 1.4d). The platform could then be attached to a mangrove root using zip ties (Fig 1.4e). Transplants were performed

by Karina Scavo Lord. The platforms used to support mangrove transplants were constructed by Jonathan Perry.

Characterizing corallite phenotypes (area, spacing, density)

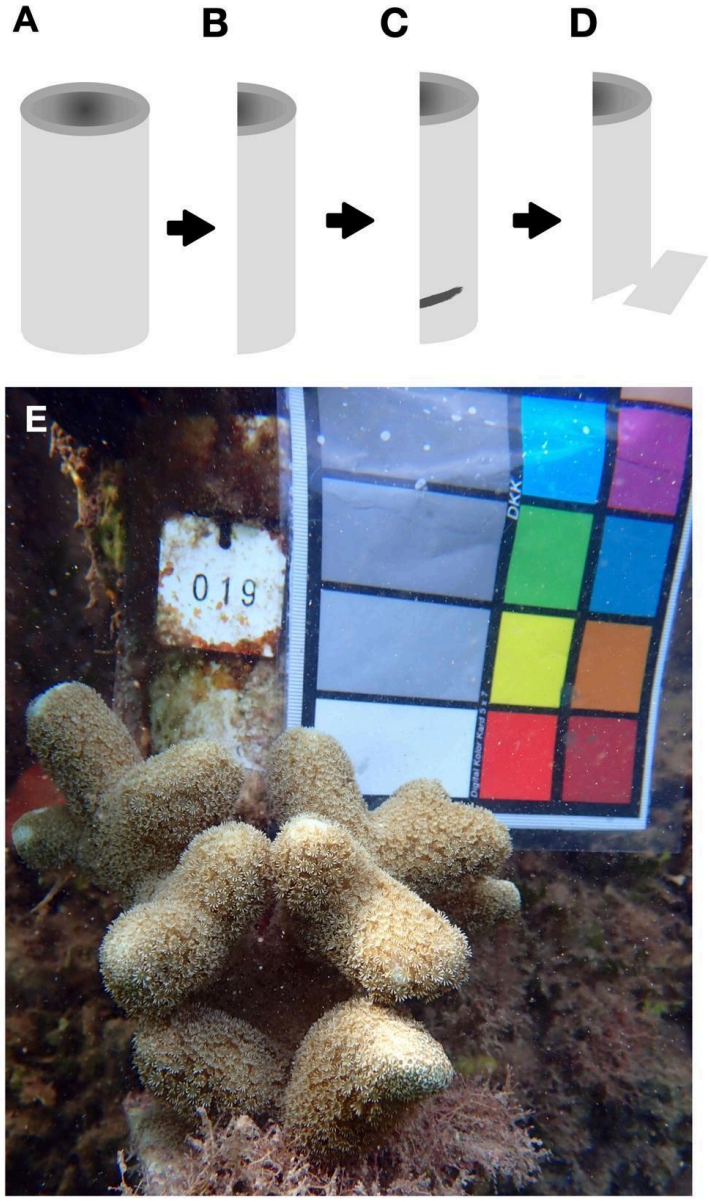

Figure 1.4. Preparation of PVC platforms to support coral transplantation onto mangrove roots (**A-D**). **E.** *Porites porites* transplant suspended on custom PCV platform, photographed two years after transplantation. The base of the PVC platform can be seen in the lower left. The upper part of the platform, which is fastened to the prop root with zip ties can be seen behind the identification tag.

Coral transplants were photographed against size and color standards and measured in situ at 30 days and 1 year after transplantation (Fig 1.4d). In December of 2019, two-years post-transplantation, all of the transplants were harvested, and tissue samples were taken for DNA and RNA analysis (Scavo Lord et al, in prep). The coral skeletons were then bleached before measurements were carried out on them. To characterize corallite size, spacing, and density, a flexible plastic stencil with known area of 0.25 cm^2 was pressed against the surface of the skeleton at multiple locations, and macro-photographs were taken. Six non-overlapping photographs were taken at widely spaced locations on each coral. Three photos were taken in areas of new growth, 1 cm below the branch tips, and three photos were taken at the base of the coral colony, in the region representing the original transplant. From these photographs (Figure 1.5a), corallite area, spacing, and density were determined. All corallites whose centers were visible within the 0.25 cm^2 stencil were counted (Figure 1.5b). Corallite density was then calculated by dividing the number of corallites by the area. Corallite area and spacing were determined from photographs using the tracing and measuring tool of ImageJ (ver. 1.53; https://imagej.net/ij/index.html) (Abramoff et al. 2004; Scavo Lord et al. 2021). Corallites falling entirely within the area delimited by the stencil were traced within each photo using the ImageJ area tracing tool (Fig 1.5c), and the area of the circumscribed corallites was calculated using the measuring tool. Corallite spacing was measured by

measuring the straight-line distances between the centers of adjacent corallites (Fig 1.5d). The average area, spacing, and density were taken for each photo.

The mean of the averaged data of corallite area, spacing, and density from the four sets of transplant locations (mangrove to mangrove, mangrove to reef, reef to reef, and reef to mangrove) were compared among tips and bases individually. Box plot and Tukey test were performed to compare the mean values in order to find the morphological differences of the original and new corallites before and after they were transplanted. If the data were significant, then P value should be less than 0.05. Each comparison was performed with and without outliers because the outliers were skewing the mean value and caused the P value to be less significant. All the results (with and without outliers) of the data analysis are in Figure 1.4 and Figure S1.

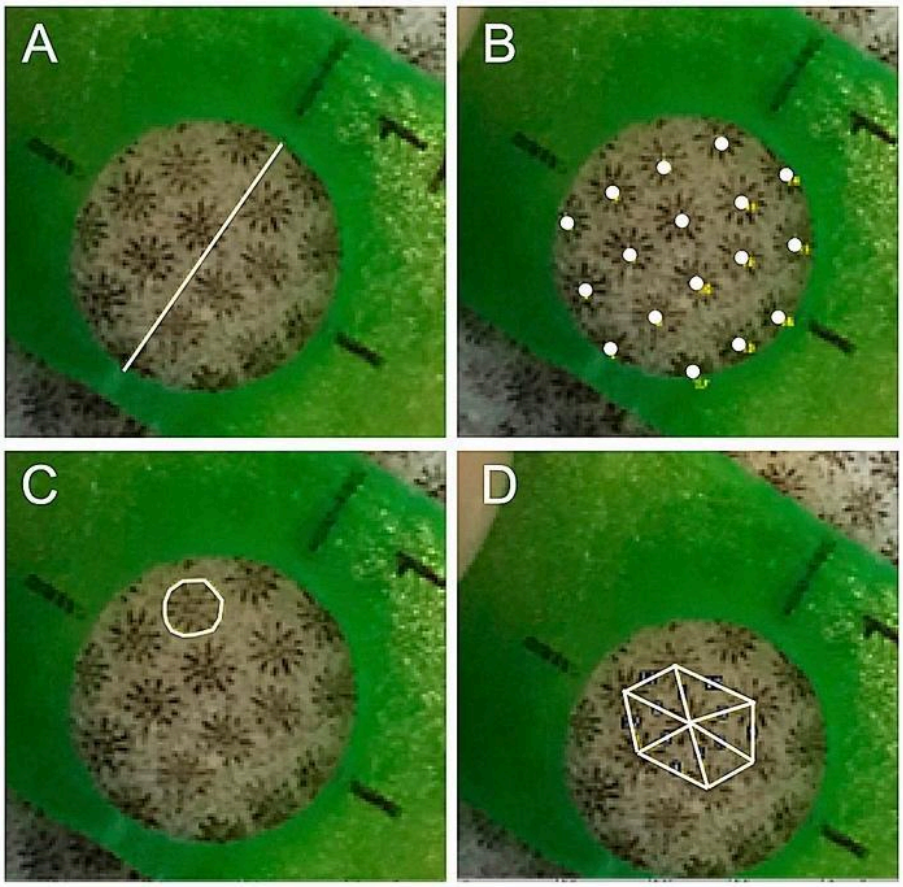

Figure 1.5. Representative photos of the corallite measurement process. **(A)** A flexible stencil of known diameter (white line) was pressed against the skeleton to circumscribe a consistent area of the coral skeleton. **(B)** All corallites whose centers (i.e., center of the columella) fall within the perimeter of the stencil are counted (white dots). **(C)** Corallite area is estimated by determining the area of the roughly circular that encloses the septa (white line). **(D)** The distance between corallites was determined by averaging the length of the line segments connecting the centers of all adjacent corallites within the stencil (e.g., white lines). All the measurements were done using ImageJ (ver. 1.53).

Results

A total of 60 coral branch tips, obtained from three mangrove corals and three reef corals, were transplanted into reef and mangrove habitats in November 2017. These transplants were scored for survival and bleaching at 30 days, one year and two years post transplantation (Scavo Lord et al., in prep; Fig. 1.6). In year two, all coral colonies were collected, the skeletons were bleached, and the corallites were scored in forty-one specimens with sufficiently intact skeletons.

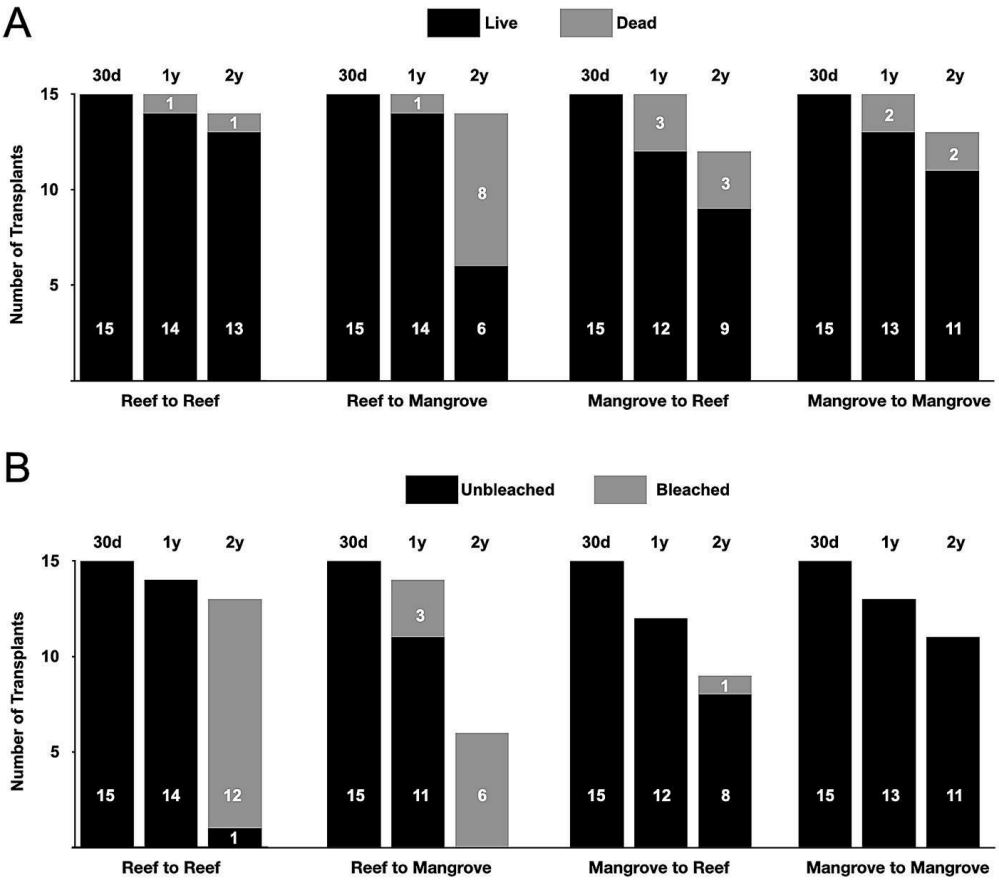

Figure 1.6. Survival **(A)** and bleaching **(B)** of coral transplants in each of the four transplant treatments (reef to reef; reef to mangrove; mangrove to reef; mangrove to mangrove) was scored by Karina Scavo Lord at 30 days, 1 year, and 2 years post-transplantation.

A total of 4,220 corallites were counted and measured from 41 coral transplants, including 2355 corallites from branch tips (new growth) and 1865 from colony bases (pre-transplant growth). On average, the density of corallites was greater in the branch tips (77.2/cm^2 ±14.4 SD) than at the base (62.2/cm^2 ±13.0 SD).

Figure 1.7 presents the mean corallite density (A,B), area (C,D) and spacing (E,F) for branch tips (A,C,E) and colony bases (B,D,F). When we focus on the effect of transplant habitat on transplants derived from the same course colony (M1-3; R1-3), except for transplants derived from M1, for which I could only measure corallite properties in one reef transplant, the average corallite density is higher for corals transplanted into the reef habitat. This is true for both the branch tips and the bases. However, none of the differences between average corallite density among transplants derived from the same source colony were statistically significant. To achieve greater corallite density, it could be the case that the corallites have a smaller area and/or that the distance between them is reduced. Particularly in the case of the branch tips, both the average area and distance between corallites tend to be smaller for those corals transplanted into the reef habitat (Fig 1.7C, E). If we compare corallite measurements of

mangrove-sourced transplants (M2,M3) versus those obtained from the reef (R1-R3), overall, the reef-sourced corals tended to have lower corallite density, greater corallite area and greater distance between adjacent corallites.

Discussion

In this study, differences in three aspects of corallite morphology were measured (area, spacing, and density) after transplanting *P. porites* between mangrove and reef habitats for a period of two years. If the corallite morphology was completely environmentally driven, then all corals being transplanted into one habitat should exhibit the same phenotype. If differences in corallite morphology are genetically or epigenetically fixed, then transplants from the same source colony should exhibit the same phenotype regardless of transplant habitat. In the present study, we found that transplanting corals from the same source colony into a reef habitat tended to result in greater corallite density, lower corallite area, and tighter corallite spacing than transplanting them into a mangrove habitat. This indicates the existence of environmental plasticity in corallite morphology. At the same time, coral transplants sourced from reef corals and mangrove corals tended to exhibit consistent differences in their response when transplanted to the same habitat. Transplants sourced from reef habitats tended to exhibit lower corallite density, greater corallite area and greater corallite spacing, regardless of whether they were transplanted back into the reef or into

the mangrove. This suggests that there may be fixed genetic or epigenetic differences between corals from different habitats.

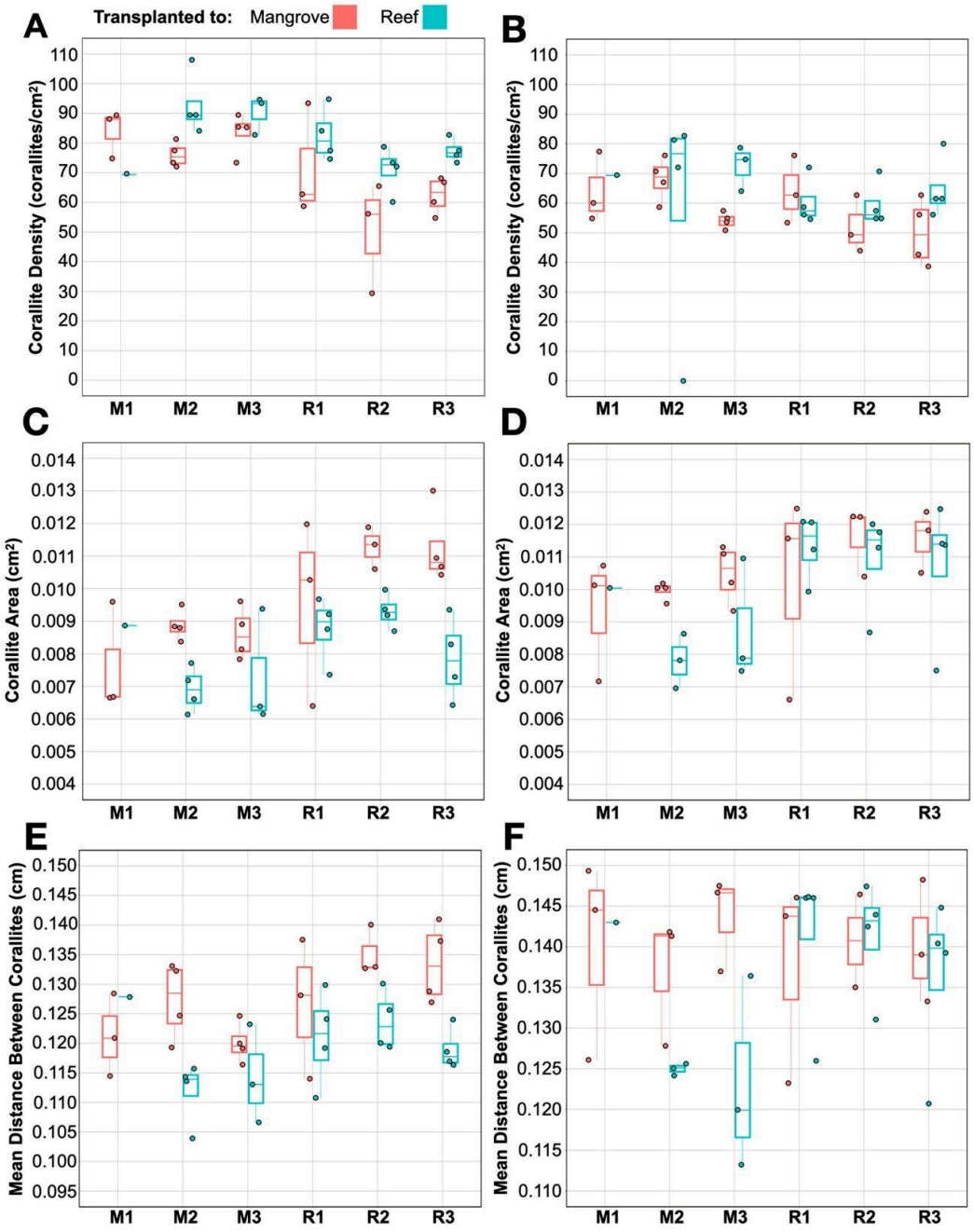

Figure 1.7. Corallite density (**A,B**), area (**C,D**), and spacing (**E,F**) in the branch tips and bases of coral transplants derived from three mangrove corals (M1-3) and three reef corals (R1-3). Individual dots represent the average of three branch tips or three locations along the colony base for coral transplants located in mangrove (red) and reef (turquoise) habitats.

Environmental differences between habitats, especially differences in light levels, are known to be associated with differences in the phenotype of coral colonies, from the overall form of the colony, to fine-scale differences in corallites (Beltran-Torres and Carricart-Gavinet 1993; Studivan et al. 2019; Scavo Lord et al. 2021). However, previous studies have generally found that corals from lower-light environments tend to have smaller corallites and greater corallite density (Studivan et al. 2019; Scavo Lord et al. 2021). For example, a previous study comparing native mangrove corals (low light) and lagoonal corals (high light), found that mangrove corals had greater corallite density and smaller corallite area (Scavo Lord et al. 2021). These results were consistent for two species in the study, both members of the same genus studied here, the thin finger coral, *Porites divaricata*, and the mustard hill coral, *P. astreoides*. As the previous study pointed out, higher corallite density has been suggested to be associated with heterotrophy in lower light environments (Scavo Lord et al. 2021). Mangroves are richer in nutrients, and consumption of nutrients such as dissolved organic carbon are important for heterotrophy and could compensate for the loss of nutrients during autotrophy in corals (Scavo Lord et al. 2021; Dittmar et al.

2006; Levas et al. 2016). The results of this study, greater corallite density and smaller corallite area in the higher light environment are therefore unexpected.

Ocean acidification has also been shown to induce changes in corallite morphology. One previous study showed that water acidification led to larger corallite area, higher porosity, and lower corallite density (Tambutté et al. 2015). Water in the mangrove habitats of the US Virgin Islands was found to be more basic (higher pH) than the water of adjacent reef habitats (Yates et al. 2014). Since higher water pH level was usually associated with warmer water (Saderne et al. 2019), this finding could potentially imply that the water temperature was higher in mangrove than reef habitats in the U.S. Virgin Islands. However, more studies are needed on what factors contributed to the morphological differences on corals between mangrove and reef habitats.

In conclusion, this study demonstrated that transplanting the Caribbean coral *P. porites* between mangrove and reef habitats on Turneffe Atoll caused corallite phenotype differences. However, in order to further understand the connection between coral morphological changes and habitats, greater replication at the level of habitats is needed, along with genetic characterization of the corals and measurements of other environmental factors such as light, pH, and temperature. More advanced corallite measuring tools would also advance future studies. I hypothesize that there is a generality of P. porites consistent morphological changes from the reef and mangrove habitats. I would like to

repeat my experiments multiple times using different branches from the same sample locations form same corals. If the findings are general, then I could isolate the contributing factors such as light and pH and further study them in more controlled laboratory settings to confirm my hypothesis.

CHAPTER TWO

VARIATION IN MICROBIOME BETWEEN MANGROVE AND REEF HABITATS OF TWO CARIBBEAN CORALS *PORITES ASTREOIDES* AND *SIDERASTREA SIDEREA*

Introduction

The microbiome is critical to the function of the coral holobiont, impacting pathogen resistance, metabolism, physiology, and nutrient cycling (Knowlton and Rohwer 2003; Olson et al. 2009; Bonthond et al. 2018). The coral microbiome consists of photosynthetic dinoflagellates of the family Symbiodiniaceae (LaJeunesse et al. 2018), in addition to other protists (e.g., *Chromium*, *Ostreobium*), bacteria, archaea, fungi, and viruses (van Oppen and Blackall 2019). The large majority of studies on the coral microbiome have focused on Symbiodiniaceae, but there has been an increasing focus on the bacterial component of the holobiont in recent years (van Oppen and Blackall 2019). However, to date, there have still been relatively few studies on other members of the holobiont, such as Archaea and protists.

Given the importance of the microbiome to the function of the coral holobiont, shifts in the microbiome can be critical in responding to environmental stress. For example, the association between coral hosts and their photosynthetic endosymbionts (Symbiodiniaceae) is known to vary due to environmental stress, including UV stress, temperature stress, and salinity stress (Baker 2003; Bonthond et al. 2018), with symbiont communities becoming reorganized after coral bleaching events (Baker 2003). The flexibility of the coral microbiome in response to stress also extends to its bacteria (McDevitt-Irwin et al. 2017; Ziegler

et al. 2019). Fewer studies have documented shifts in the coral archaeal or protist communities in response to environmental stress, although, in one recent study, the archaeal community experienced relative stasis as the bacterial community shifted significantly in a coral under heat stress (Ju et al. 2024).

As reef and lagoon habitats differ dramatically with respect to key environmental variables such as light levels and temperature variability (Camp et al. 2016; Scavo Lord et al. 2021), generalist corals that are able to thrive in both habitats must adjust their physiology and metabolism. Some part of this adjustment may come through a change in the composition of the microbiome. To understand the differences in the coral microbiome across mangrove and reef habitats, we used 16S-based metagenomics to compare the diversity and abundance of Bacteria, and Archaea as well as eukaryotic mitochondria and chloroplasts in two widespread Caribbean corals, the mustard hill coral, *Porites astreoides*, and the massive starlet coral, *Siderastrea siderea*. *P. astreoides* is a brooding coral that has been shown to vertically transmit bacteria in its larvae and exhibit little geographic variability in the composition of its microbiome (Wegley et al. 2007; Rodriguez-Lanetty et al. 2013; Meyer et al. 2014). Healthy *P. astreoides* were found to harbor abundant Rhodobacterales, Alteromonadales, Rhizobiales, and Cyanobacteria (Wegley et al. 2007; Rodriguez-Lanetty et al. 2013; Meyer et al. 2014). *S. siderea,* by contrast to *P. astreoides*, is a broadcast spawner (Lirman & Fong 2007; Bonthond et al. 2018). However, like *P.*

astreoides, *S. siderea* is among the most resilient corals in the face of environmental fluctuations on Caribbean reefs (Bove et al. 2019; Aichelman et al. 2021), and it is also found in both reef and mangrove habitats (Hernández Fernández 2015; Rogers 2017; Bengtsson et al. 2019). The microbiome of *S. siderea* has been shown to exhibit substantial shifts in response to environmental variation (Bonthond et al. 2018; Wang et al. 2018; Alvarez-Yela et al. 2019; Speare et al. 2020; Howard et al. 2023).

As part of a larger metagenomic project comparing the microbiome of *P. astreoides* and *S. siderea* across mangrove and lagoon habitats (Lee, Scavo Lord, et al., in prep), in the research described in this chapter, I investigated 16S sequences that appeared to derive from Archaea, mitochondria, and eukaryotic chloroplasts. While the number of distinct archaeal and chloroplast "amplified sequence variants" (ASVs) recovered was substantially smaller than the number of bacterial ASVs, I was able to identify archaeal and chloroplasts comprising part of the core microbiome of either *P. astreoides* or *S. siderea*, and I was able to identify significant archaeal or chloroplast indicator species that were associated with one of the four species x habitat combinations. None of the small number of eukaryotic mitochondrial sequences appeared to be part of the core microbiome of either coral. Nor did any of the mitochondrial sequences appear among the indicator species.

Materials and methods

Note: The research I conducted on archaeal and chloroplasts sequences is embedded within a larger study. As my thesis research cannot be disentangled from this broader project, the entire data generation and analysis pipeline is provided below, including aspects of the research that were performed by my collaborators. The methods presented below are modified from a manuscript in preparation on which I am a co-author (Lee, Scavo Lord, et al., in prep).

Study site and coral collection

Field sampling was performed by John Finnerty, Karina Scavo Lord, and Hannah Aichelman. Tissue samples were obtained from ten spatially discrete *S. siderea* colonies, five from Crooked Creek (Fig 2.2 a-e) and five from Central Lagoon (Fig 2.3 a-e) and ten spatially discrete *P. astreoides* colonies, five from Crooked Creek (Fig 2.2 f-j) and five from Central Lagoon (Fig 2.3 f-j). At the time of tissue sampling, all corals were photographed *in situ*, both alone and against a size and color standard (Fig. 2.2; 2.3). All *P. astreoides* in Crooked Creek were growing as epibionts upon the prop roots of red mangrove (*Rhizophora mangle*). Likewise, two *S. siderea* from Crooked Creek were growing as mangrove epibionts. The other three *S. siderea* were located beneath the mangrove canopy, growing upon the underlying peat bank. Hammer and chisel were used to obtain a fragment, approximately 0.5 cm^3 in volume, from

each coral. This fragment was immediately placed in a 5-ml microcentrifuge tube containing 100% ethanol. Upon return to the Calabash Caye Field Station, the fragments were placed in fresh ethanol and stored at -20°C. The collection tubes were transported back to Boston University in a liquid nitrogen dry-shipper. All samples were collected on December 16, 2018, during a one-hour period (approximately 1:40-2:40 pm).

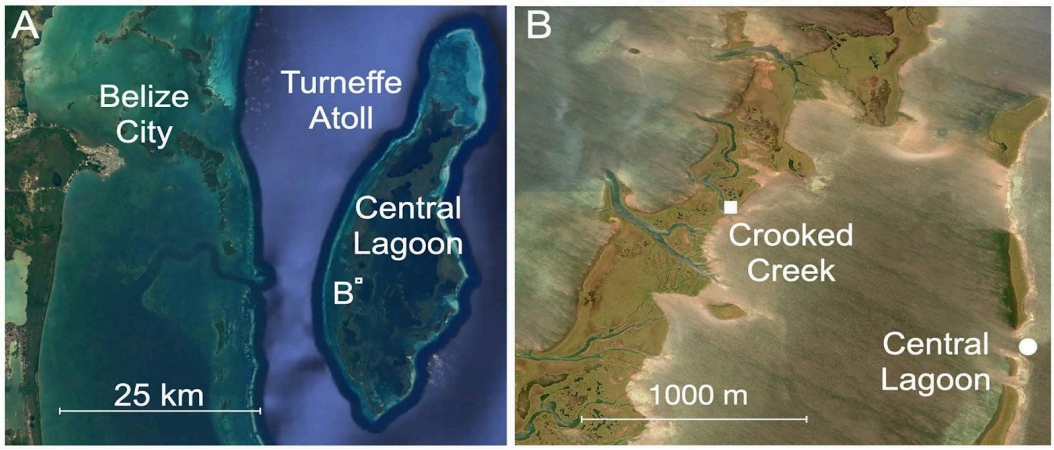

Figure 2.1. Location of study sites on Turneffe Atoll, Belize. (A) Turneffe Atoll in relation to the shoreline of the Belizean mainland. (B) Crooked Creek and adjacent region of Central Lagoon. The approximate center of the shoreline in Crooked Creek where corals were sampled (white square) is 17°19'46.32"N and 87°55'6.40"W. The approximate center of the Central Lagoon site where corals were sampled (white circle) is located at 17°19'37.95"N and 87°54'59.61"W. The image is dated April 12, 2009 and was obtained using Google Earth Pro (v 7.3.4.8248). Image © 2021 Maxar Technologies. Figure preparation by John R. Finnerty.

DNA isolation, library preparation, and sequencing

DNA extraction and library preparation were performed by myself and fellow students enrolled in the 2022 offering of Professor Finnerty's *Marine Genomics* course, under the direction of Joanna C. Lee and Karina Scavo Lord. DNA was extracted from ~100 mg of each coral sample, consisting of a skeleton with overlying tissue, that was first broken down into small fragments using a razor blade. DNA was extracted using the DNeasy Blood and Tissue Kit (Qiagen) according to the manufacturer's specifications. Libraries for Illumina sequencing sequencing were then constructed using two rounds of PCR with overlapping primer sets (Fig. 2.4). Round one used primers incorporating a 19-20 nt degenerate region specific to the V4 region of 16S ribosomal DNA fused to adaptors that would serve as the site of priming for the second round of PCR. These previously published primers are known as Hyb515f and Hyb806r (Apprill et al. 2015; Parada et al. 2016). Following the first round of PCR, primers and unincorporated nucleotides were removed using the GeneClean PCR cleanup kit (MP Biomedical). The second round of PCR utilized primers that overlapped with the adaptors incorporated in round one, but added unique 6-nt barcodes as well as a sequencing adaptor that would allow the fragments to bind to the flow cell and be sequenced (Figure 2.4). Through a combination of twelve distinct barcodes on the forward primers and eight distinct barcodes on the reverse

primers (Figure 2.4), 96 unique 16S libraries could be sequenced on a single flow cell. PCR thermocycling profiles are provided in Figure 2.4. Following the second round of PCR, primers and unincorporated nucleotides were again removed using the GeneClean kit. Samples were pooled and sequencing was performed by Novogene on an Illumina HiSeq using paired 250-bp reads. For each DNA sample, libraries were constructed in triplicate, so that we could assess the repeatability. Negative controls using water in place of DNA template were also performed in triplicate.

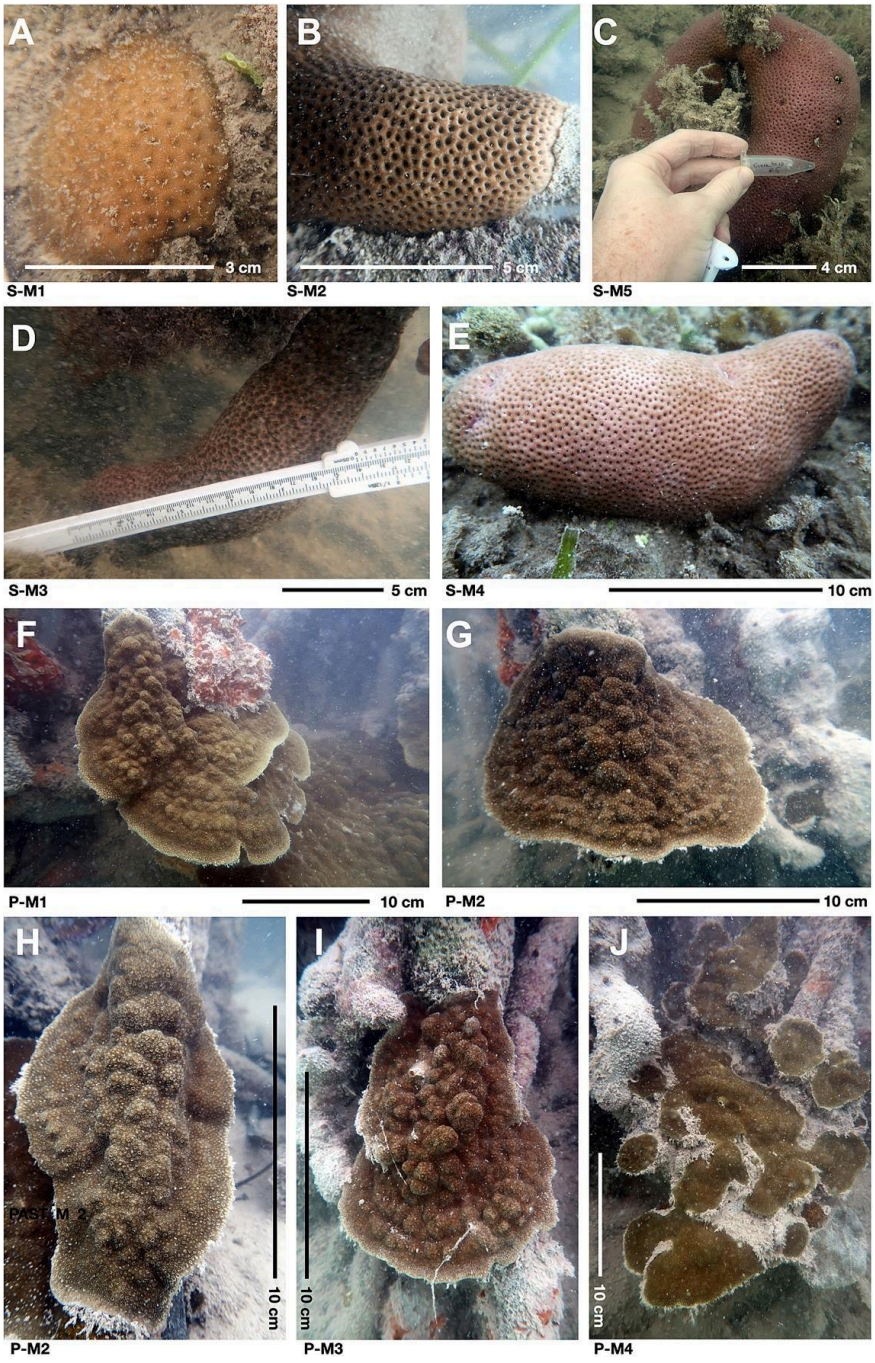

Figure 2.2. Corals sampled from Crooked Creek. **(A-E)** *Siderastrea siderea*. **(F-J)** *Porites astreoides*. Photos and figures by John R. Finnerty.

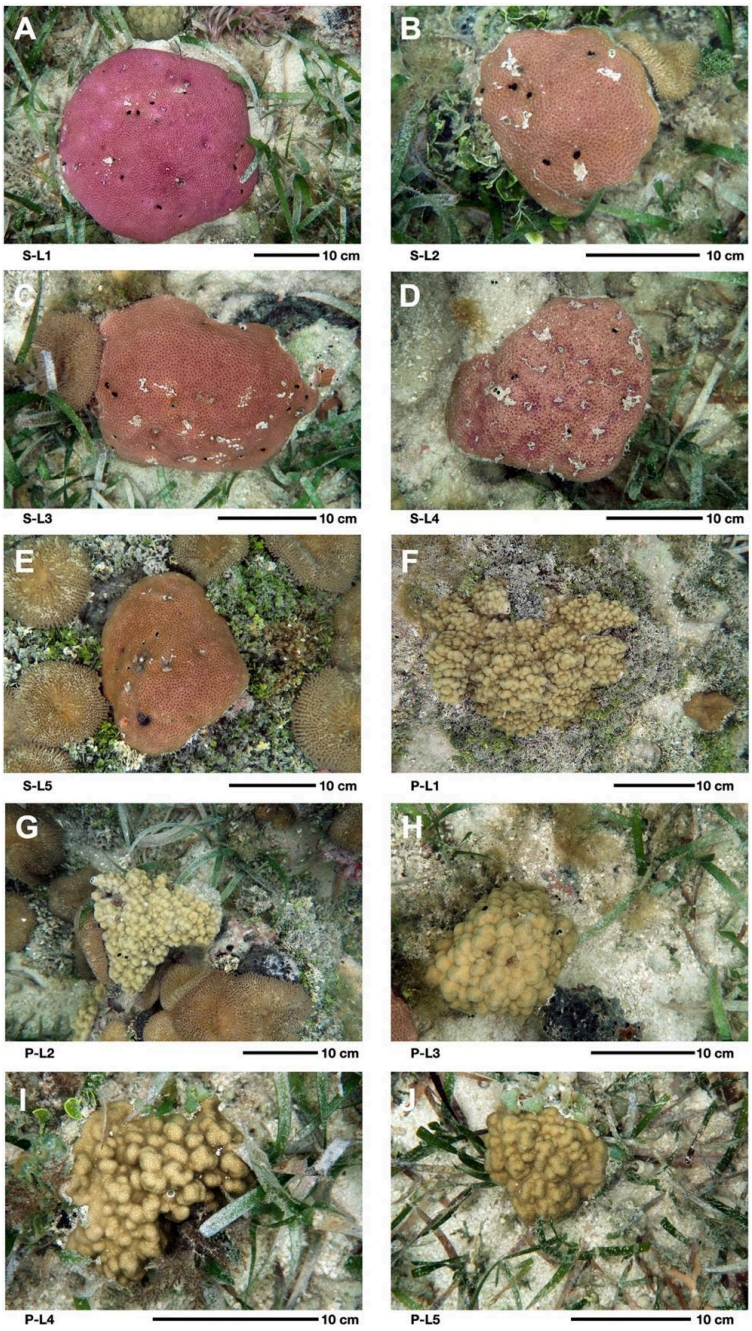

Figure 2.3. Corals sampled from Central Lagoon. **(A-E)** *Siderastrea siderea*. **(F-J)** *Porites astreoides*. Photos and figures by John R. Finnerty.

PRIMER	SEQUENCE	REF
16S primers		
Hyb515F	5′-TCGTCGGCAGCGTCAGATGTGTATAAGAGACAGNNNNGTGYCAGCMGCCGCGGTAA-3′	Apprill *et al.*, (2015); Parada *et al.* (2016);
Hyb806R	5′-GTCTCGTGGGCTCGGAGATGTGTATAAGAGACAGNNNNGGACTACNVGGGTWTCTAAT-3′	Apprill *et al.*, (2015); Parada *et al.* (2016);
Adaptor-primers		
Hyb_F13_i5	5′-AATGATACGGCGACCACCGAGATCTACACAGTCAATCGTCGGCAGCGTC-3′	
Hyb_F14_i5	5′-AATGATACGGCGACCACCGAGATCTACACAGTTCCTCGTCGGCAGCGTC-3′	
Hyb_F16_i5	5′-AATGATACGGCGACCACCGAGATCTACACCCGTCCTCGTCGGCAGCGTC-3′	
Hyb_F17_i5	5′-AATGATACGGCGACCACCGAGATCTACACGTAGAGTCGTCGGCAGCGTC-3′	
Hyb_F19_i5	5′-AATGATACGGCGACCACCGAGATCTACACGTGAAATCGTCGGCAGCGTC-3′	
Hyb_F20_i5	5′-AATGATACGGCGACCACCGAGATCTACACGTGGCCTCGTCGGCAGCGTC-3′	
Hyb_F22_i5	5′-AATGATACGGCGACCACCGAGATCTACACCGTACGTCGTCGGCAGCGTC-3′	
Hyb_F23_i5	5′-AATGATACGGCGACCACCGAGATCTACACGAGTGGTCGTCGGCAGCGTC-3′	
Hyb_F25_i5	5′-AATGATACGGCGACCACCGAGATCTACACACTGATTCGTCGGCAGCGTC-3′	
Hyb_F27_i5	5′-AATGATACGGCGACCACCGAGATCTACACATTCCTTCGTCGGCAGCGTC-3′	
Hyb_F29_i5	5′-AATGATACGGCGACCACCGAGATCTACACCAACTATCGTCGGCAGCGTC-3′	
Hyb_F31_i5	5′-AATGATACGGCGACCACCGAGATCTACACCACGATTCGTCGGCAGCGTC-3′	
Hyb_R43_i7	5′-CAAGCAGAAGACGGCATACGAGATGCTGTAGTCTCGTGGGCTCGG-3′	
Hyb_R48_i7	5′-CAAGCAGAAGACGGCATACGAGATTGCCGAGTCTCGTGGGCTCGG-3′	
Hyb_R46_i7	5′-CAAGCAGAAGACGGCATACGAGATTCGGGAGTCTCGTGGGCTCGG-3′	
Hyb_R45_i7	5′-CAAGCAGAAGACGGCATACGAGATGAATGAGTCTCGTGGGCTCGG-3′	
Hyb_R44_i7	5′-CAAGCAGAAGACGGCATACGAGATATTATAGTCTCGTGGGCTCGG-3′	
Hyb_R41_i7	5′-CAAGCAGAAGACGGCATACGAGATGTCGTCGTCTCGTGGGCTCGG-3′	
Hyb_R40_i7	5′-CAAGCAGAAGACGGCATACGAGATTCTGAGGTCTCGTGGGCTCGG-3′	
Hyb_R39_i7	5′-CAAGCAGAAGACGGCATACGAGATGTATAGGTCTCGTGGGCTCGG-3′	

Gene specific Adaptor tails Barcodes

PCR REACTIONS

AMPLICON	FORWARD PRIMER	REVERSE PRIMER	TEMPLATE	THERMOCYCLING PARAMETERS	LENGTH (nt)
16S rDNA	Hyb515F	Hyb806R	gDNA	95°C/10 min; 30x: 95°C/40 s, 58°C/2 min, 72°C/1 min; 72°C/10 min	~376
16S Library	Hyb_F##_i5	Hyb_R##_i7	16S rDNA amplicons	95°C/5 min; 5x: 95°C/40 s, 59°C/2 min, 72°C/1 min; 72°C/7 min	~471

Figure 2.4. Primers and PCR thermocycling profiles used to generate 16S libraries.

Data generation and processing workflow

The 16S data generation and processing pipeline is depicted in Figure 2.5. Data processing was performed by Joanna C. Lee using the following steps. Following primer/adapter removal and the matching of paired reads, *dada2,* v. 1.20.0 (Callahan et al. 2016) was used to process the resulting 16S sequences. First, the *plotQualityProfile* function was used to inspect the read quality profiles. Then, using the *filterandTrim* function, reads less than 200 nt, and reads with ≥1

expected error were discarded, and based upon the read quality profiles, the first 25 nt at the start of each remaining read were removed. The *learnErrors* and *plotErrors* functions were then used to estimate error rates and determine if PCR/sequencing errors followed expected patterns. The *derepFastq* function was then used to combine identical sequencing reads, and *mergePairs* was used to merge paired forward and reverse sequencing reads. Distinct amplified sequence variants (ASVs) were then inferred from the duplicated reads using the standard *dada2* algorithm (Callahan et al. 2016) and formatted into an ASV sequence table. The *assignTaxonomy* function was then used in combination with the "silva_nr_v132_train_set.fa" database to assign ASVs to the finest taxonomic level possible, down to the presumptive genus. Where possible, the *addSpecies* function was used in combination with the "silva_species_assignment_v132.fa" database to assign species identifications. All ASVs were then sorted into bacterial, archaeal, chloroplast, and mitochondrial bins, while removing ASVs that could not be identified at any taxonomic level. These presumptive bacterial, archael, chloroplast, and mitochondrial ASVs were then used to query the non-redundant (nr) nucleotide database at NCBI using *BLASTn*, and all sequences that exhibited a top hit to something other than the taxonomic bin into which they were assigned by *dada2*'s *assignTaxonomy* function were discarded. Finally, we removed ASVs that were only recovered in a single coral colony, regardless of their overall relative abundance, and we removed ASVs exhibiting a relative

abundance <0.001. ASVs were covered in the negative controls were removed from all the samples.

Comparison of microbiome composition between sites and species

The Shannon Diversity Index (*H*) of bacterial, archaeal and chloroplast ASVs was computed for each sample using the estimate_richness function of *phyloseq, v. 1.36.0.* The mean value of *H* was then plotted for each species in each habitat using the *ggplot* function of *ggplot2* v. 3.3.5. The Student's t-test was used to test for differences in average diversity between mangrove and lagoon populations of each species and between all mangrove samples and all lagoon samples.

Differences in bacterial, archaeal, and chloroplast composition among sites and species were assessed as follows. First, raw ASV count data for all samples were transformed to relative abundance using the *"transform_sample_counts"* function. Bray Curtis dissimilarity distances were then calculated between all samples, and significant variation in ASV richness and abundance between the two coral species, habitats, and species-by-habitat combinations (PAST/mangrove, PAST/lagoon, SSID/mangrove, SSID/lagoon) were assessed using a PERMANOVA with the *adonis2* function of the *vegan* R package, with the number of permutations set to 9999 (De Cáceres and Legendre

2009). Finally, pairwise Bray Curtis distances were plotted according to the NMDS ordination method using the *ordinate* function in *phyloseq*.

Finally, we identified the core microbiome in each species as well as indicator ASVs for each of the four species-by-site combinations. Core microbiota — those ASVs shared by $\geq$ 70% of individuals within a species—were identified for *P. astreoides* and *S. siderea* using the *microbiome* R package (Lahti and Shetty 2017). After grouping samples into the four species/site combinations, bacterial, archaeal, and chloroplast "indicator species" were detected with the *multipatt* function in the *indicspecies* R package (De Cáceres et al. 2010) using the IndVal.g association function with 9999 permutations. Indicator ASVs were retained if they had an indicator value, $I > 0.3$ and $p < 0.05$.

SEQUENCING

Habitat	MANGROVE		LAGOON	
Species	*Porites astreoides*	*Siderastrea siderea*	*Porites astreoides*	*Siderastrea siderea*
Colonies	3	4	4	4
PCR replicates per colony	3	3	3	3
Read Length	2 x 250bp	2 x 250bp	2 x 250bp	2 x 250bp

RAW SEQUENCING READS

	# READS
TOTAL	18,197,880
AVG	404,397
STDEV	335,939

SAMPLE	# READS	SAMPLE	# READS	SAMPLE	# READS	SAMPLE	# READS
P-M2 A	280,904	S-M1 A	1,412,762	P-L1 A	224,296	S-L1 A	743,570
P-M2 B	431,608	S-M1 B	1,182,906	P-L1 B	332,532	S-L1 B	1,158,938
P-M2 C	243,950	S-M1 C	289,656	P-L1 C	503,312	S-L1 C	1,054,586
P-M3 A	317,536	S-M2 A	784,490	P-L2 A	230,784	S-L2 A	242,532
P-M3 B	820,388	S-M2 B	470,984	P-L2 B	415,842	S-L2 B	7,546
P-M3 C	833,992	S-M2 C	444,768	P-L2 C	553,208	S-L2 C	609,630
P-M4 A	234,666	S-M3 A	105,038	P-L3 A	215,950	S-L3 A	4,242
P-M4 B	268,250	S-M3 B	139,104	P-L3 B	358,552	S-L3 B	185,716
P-M4 C	456,916	S-M3 C	127,010	P-L3 C	244,014	S-L3 C	632
		S-M5 A	210,422	P-L4 A	749,390	S-L4 A	45,688
		S-M5 B	319,770	P-L4 B	433,168	S-L4 B	80,010
		S-M5 C	172,472	P-L4 C	208,850	S-L4 C	47,300
AVERAGE	432,023	AVERAGE	471,615	AVERAGE	372,492	AVERAGE	348,366
STDEV	237,201	STDEV	433,576	STD	167,606	STD	429,338

FILTERED SEQUENCING READS

(1) Trim 25nt from start of reads. (2) Discard reads < 200nt & with ≥1 expected error.

	# READS
TOTAL	15,061,170
AVG	334,693
STDEV	268,872

SAMPLE	# READS	SAMPLE	# READS	SAMPLE	# READS	SAMPLE	# READS
P-M2 A	234,604	S-M1 A	1,137,018	P-L1 A	210,000	S-L1 A	632,652
P-M2 B	354,720	S-M1 B	951,436	P-L1 B	313,134	S-L1 B	958,406
P-M2 C	195,876	S-M1 C	227,614	P-L1 C	465,040	S-L1 C	864,840
P-M3 A	265,164	S-M2 A	584,208	P-L2 A	209,560	S-L2 A	218,462
P-M3 B	630,206	S-M2 B	352,118	P-L2 B	373,038	S-L2 B	6,402
P-M3 C	583,334	S-M2 C	327,356	P-L2 C	484,324	S-L2 C	522,322
P-M4 A	204,992	S-M3 A	92,520	P-L3 A	186,500	S-L3 A	3,046
P-M4 B	222,160	S-M3 B	121,856	P-L3 B	312,346	S-L3 B	162,026
P-M4 C	385,082	S-M3 C	109,186	P-L3 C	198,406	S-L3 C	236
		S-M5 A	186,588	P-L4 A	652,018	S-L4 A	40,536
		S-M5 B	278,040	P-L4 B	369,554	S-L4 B	65,992
		S-M5 C	152,788	P-L4 C	177,408	S-L4 C	38,056
AVERAGE	341,793	AVERAGE	376,727	AVERAGE	329,277	AVERAGE	292,748
STDEV	164,029	STDEV	342,452	STD	147,665	STD	355,811

AMPLICON SEQUENCE VARIANTS (ASVs)

(3) Merge forward & reverse reads

	# ASVs
TOTAL	11,202,900
AVG	248,953
STDEV	236,298

SAMPLE	# ASVs	SAMPLE	# ASVs	SAMPLE	# ASVs	SAMPLE	# ASVs
P-M2 A	144,126	S-M1 A	985,546	P-L1 A	25,830	S-L1 A	556,694
P-M2 B	200,682	S-M1 B	823,752	P-L1 B	36,492	S-L1 B	810,024
P-M2 C	103,060	S-M1 C	207,092	P-L1 C	90,082	S-L1 C	717,906
P-M3 A	242,754	S-M2 A	534,052	P-L2 A	178,230	S-L2 A	205,310
P-M3 B	511,726	S-M2 B	330,410	P-L2 B	269,866	S-L2 B	6,282
P-M3 C	462,466	S-M2 C	310,078	P-L2 C	387,898	S-L2 C	458,812
P-M4 A	100,798	S-M3 A	86,760	P-L3 A	89,850	S-L3 A	2,958
P-M4 B	151,004	S-M3 B	111,778	P-L3 B	154,288	S-L3 B	150,760
P-M4 C	231,576	S-M3 C	101,136	P-L3 C	109,844	S-L3 C	226
		S-M5 A	167,110	P-L4 A	339,928	S-L4 A	39,896
		S-M5 B	240,558	P-L4 B	194,616	S-L4 B	64,390
		S-M5 C	134,432	P-L4 C	94,556	S-L4 C	37,266
AVG	238,688	AVG	336,059	AVG	164,290	AVG	254,210
STDEV	150,074	STDEV	295,754	STDEV	115,832	STDEV	299,776

DISTINCT AMPLICON SEQUENCE VARIANTS (ASVs)

(4) Consolidate identical reads. (5) Assign taxonomy to 17325 distinct ASVs using (a) silva_nr_v132_train_set.fa, (b) silva_species_assignment_v132.fa, and (c) NCBI BLAST. (6) Eliminate ASVs below a relative abundance of 0.001% (n=14395), and ASVs only present in only one sample (n=766); (7) Segregate ASVs by taxonomic bin: Bacteria (1055); Archaea (604); chloroplasts (200), mitochondria (171), Eukaryota (58), unidentified sequences (76).

Bacterial ASVs	1,055
Avg. ASVs / Sample	202.3
+/- St. Dev.	120.2
Avg. Counts / ASV	262.3
+/- St. Dev.	252.7

Archaeal ASVs	604
Avg. ASVs / Sample	29.1
+/- St. Dev.	42.1
Avg. Counts / ASV	257.6
+/- St. Dev.	436.7

Chloroplast ASVs	200
Avg. ASVs / Sample	17.6
+/- St. Dev.	9.7
Avg. Counts / ASV	3,093.4
+/- St. Dev.	2,749.5

SAMPLE	Bac	Arc	Chl	SAMPLE	Bac	Arc	Chl	SAMPLE	Bac	Arc	Chl	SAMPLE	Bac	Arc	Chl
P-M2 A	258	12	21	S-M1 A	361	196	45	P-L1 A	17	1	11	S-L1 A	379	36	28
P-M2 B	284	23	25	S-M1 B	337	168	42	P-L1 B	16	0	6	S-L1 B	421	43	32
P-M2 C	227	10	16	S-M1 C	212	76	22	P-L1 C	23	2	7	S-L1 C	408	44	32
P-M3 A	256	14	17	S-M2 A	351	107	32	P-L2 A	87	2	7	S-L2 A	173	17	16
P-M3 B	322	21	20	S-M2 B	318	62	24	P-L2 B	97	2	7	S-L2 B			
P-M3 C	316	17	18	S-M2 C	310	73	28	P-L2 C	125	2	10	S-L2 C	213	14	18
P-M4 A	202	6	16	S-M3 A	69	2	8	P-L3 A	212	31	20	S-L3 A			
P-M4 B	234	9	15	S-M3 B	80	5	4	P-L3 B	271	37	24	S-L3 B	101	15	11
P-M4 C	260	10	20	S-M3 C	79	3	10	P-L3 C	217	31	20	S-L3 C			
				S-M5 A	53	2	8	P-L4 A	357	48	26	S-L4 A	60	6	7
				S-M5 B	70	11	15	P-L4 B	282	35	16	S-L4 B	75	3	7
				S-M5 C	68	4	7	P-L4 C	218	16	15	S-L4 C	78	5	6
AVG	262	14	19	AVG	192	59	20	AVG	160	17	14	AVG	212	20	17
STDEV	40	6	3	STDEV	133	68	14	STDEV	115	18	7	STDEV	152	16	11

Figure 2.5. 16S data generation and data processing pipeline.

Results

Recovery of 16S sequence variants

We obtained a total of 18,197,880 raw sequencing reads from 15 coral colonies: four *S. siderea* colonies from both lagoon and mangrove, four *P. astreoides* colonies from lagoon, and three *P. astreoides* colonies from mangrove (Fig. 2.5). For each colony, we sequenced three PCR replicates. After discarding reads <200 nt and those with ≥1 expected error, an average of ~335,000 sequence reads were obtained per sample (Fig. 2.5). However, for three replicates—all *S. siderea* samples from the lagoon—relatively few reads were obtained, and these samples were therefore excluded from subsequent analyses.

After merging forward and reverse reads, consolidating identical sequences, and eliminating rare sequence variants (relative abundance <0.001%) as well as those unique to a single coral colony, we were left with 1055 distinct bacterial amplified sequence variants, 604 archaeal ASVs, and 200 chloroplast ASVs (Fig. 2.5). My analyses focused on Archaea and chloroplasts, but results for Bacteria are included here for context.

The 1055 distinct bacterial sequences recovered in this study were assigned to 29 different phyla, with six phyla accounting for almost 90% of all ASVs: Proteobacteria (n=566), Bacteroidetes (166), Planctomycetes (87), Chiroflexi (65), Acidobacteria (32), and Actinobacteria (27). On average, we recovered 202.3 ± 120.2 distinct bacterial ASVs per sample, with each ASV being

sequenced an average of 262.3 times. Replicate samples tended to exhibit similar proportions of bacterial classes, indicating a high degree of technical reproducibility (Fig. 2.6).

The 604 distinct archaeal sequences recovered in this study were assigned to 6 different phyla. In decreasing order of abundance, these were Nanoarchaeaeota (n=393), Thaumarchaeota (95), Euryarchaeota (38),

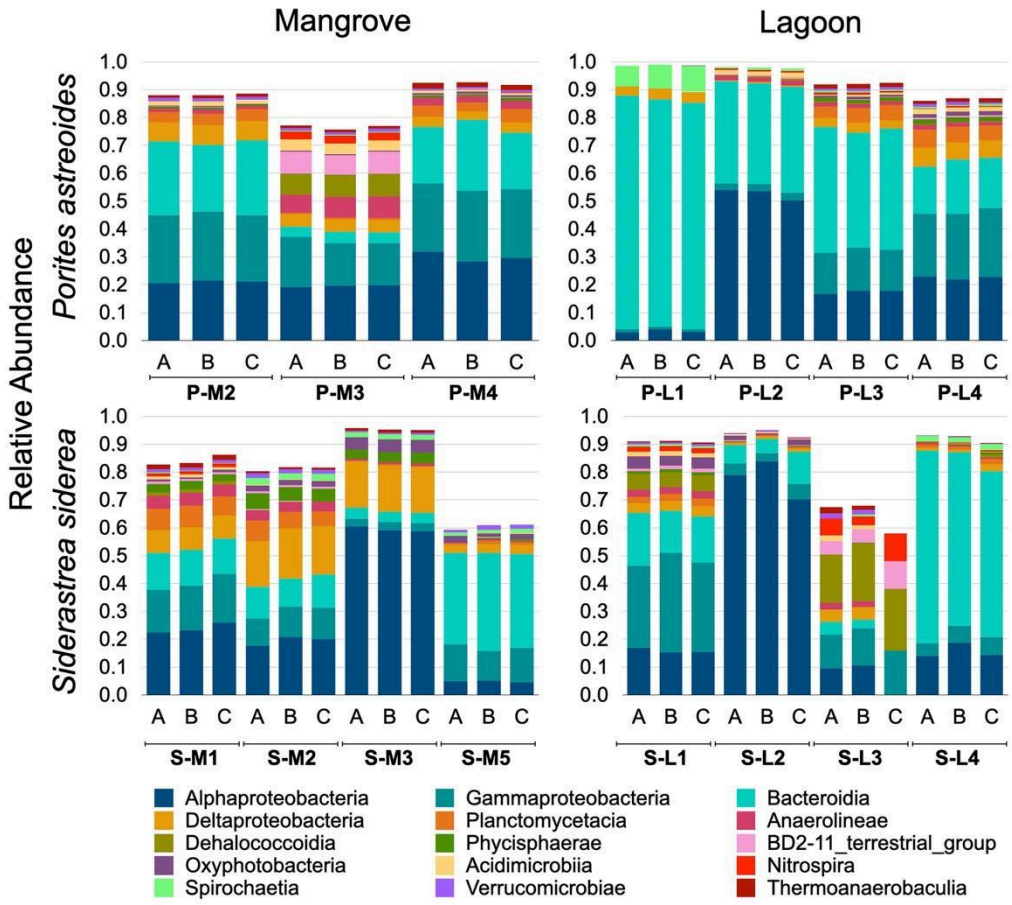

Figure 2.6. Relative proportion of bacterial classes represented by ASVs from *P. astreoides* and *S. siderea* mangrove and lagoon corals. Replicate samples are indicated by the letters A-C above the coral colony names (e.g., P-M2).

Asgardaeota (16), Crenarchaeota (16), and Diapherotrites (3). Forty-three ASVs could not be assigned to a phylum within Archaea. Individual samples had an average of 27.6 ± 42.2 distinct archaeal ASVs (Fig. 2.5), with each ASV being sequenced an average of 257.6 times. Replicate samples tended to exhibit similar proportions of archaeal phyla (Fig. 2.7).

Two-hundred distinct chloroplast sequences were recovered in this study. Individual samples harbored 17.6 ± 9.7 distinct chloroplast ASVs on average (Fig. 2.5). These chloroplast ASVs were sequenced 3,093.4 times per sample, on average. Blast searches of the NCBI non-redundant nucleotide database indicate that some of these chloroplast sequences belong to *Ostreobium*, a genus of endolithic green algae known to inhabit coral skeletons (del Campo et al. 2016).

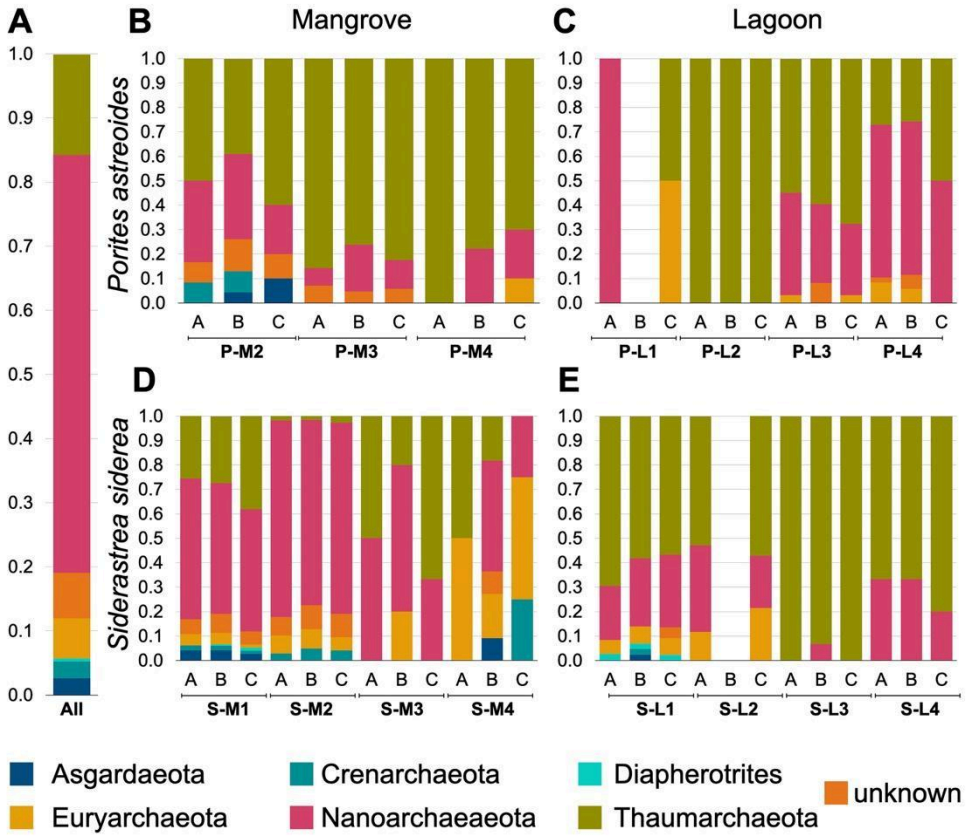

Figure 2.7. Relative proportion of archaeal phyla represented by ASVs from *P. astreoides* and *S. siderea* mangrove and lagoon corals. Replicate samples are indicated by the letters A-C above the coral colony names (e.g., P-M2).

Microbiome comparison between species and habitats

In general, there was no difference in overall diversity of bacterial, archaeal, and chloroplast sequences between *P. astreoides* and *S. siderea* from mangrove and lagoon habitats based upon the Shannon diversity index (Fig. 2.8). The only significant difference was between the chloroplast diversity of *P.*

astreoides and *S. siderea* from mangrove habitats, with the mustard hill coral exhibiting higher diversity (Fig. 2.6c).

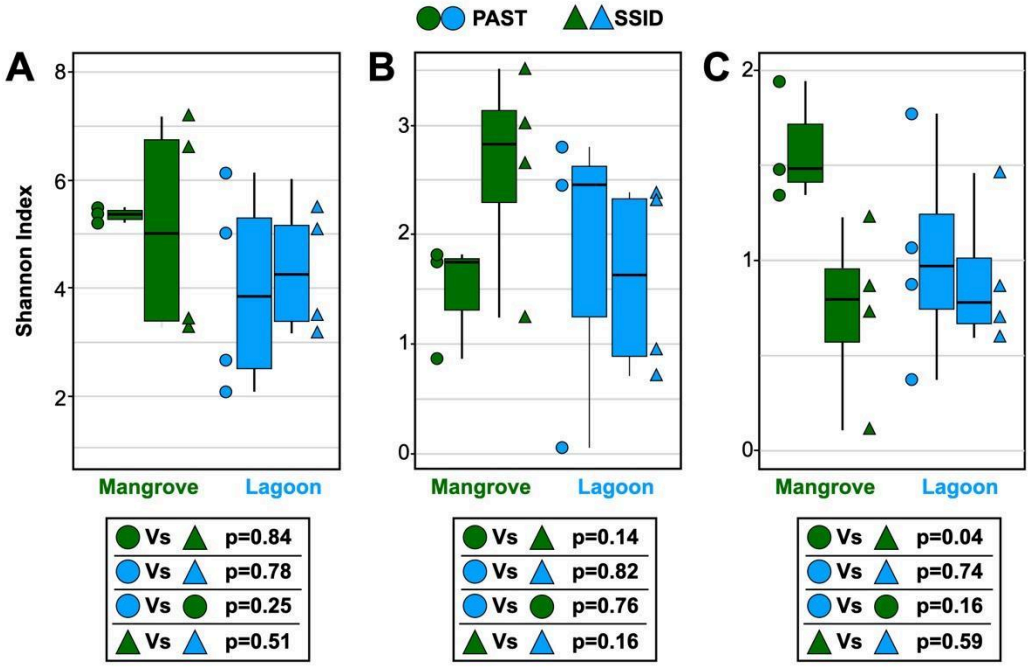

Figure 2.8. Comparison of Shannon diversity index between *P. astreoides* and *S. siderea* in mangrove and lagoon habitats for (A) bacteria, (B) archaea, and (C) chloroplast ASVs. Circles represent the average of three replicates for the seven P. astreoides and triangles represent the average of three replicates for the eight S. siderastrea sampled in this study.

Consistent with the similarity in the proportions of bacterial classes and archaeal phyla shown in Figures 2.6 and 2.7, non-metric dimensional scaling analyses (NMDS) show tight grouping of replicate samples based upon either their bacterial, archaeal, or chloroplast ASV abundances (Figures 2.9, 2.10, 2.11). After averaging the relative abundances of all ASVs across replicate samples

from the same coral, NMDS analyses suggest that the most pronounced differences in bacterial assemblages may be found between *P. astreoides* from mangrove and lagoon (Fig. 2.9 b,c), *S. siderea* from mangrove and lagoon (Fig. 2.9 b,d), and *P. astreoides* and *S. siderea* from the mangrove (Fig. 2.9 b,e). By contrast, the NMDS plots reveal greater overlap between the bacterial communities of *P. astreoides* and *S. siderea* from the lagoon (Fig. 2.9 b,f). However, only the difference between *P. astreoides* and *S. siderea* from the mangrove approaches statistical significance (Fig. 2.9 f; $p=0.057$). The NMDS analysis for Archaea (Fig. 2-10) fails to differentiate samples by species, by site, or by the combination of species and site.

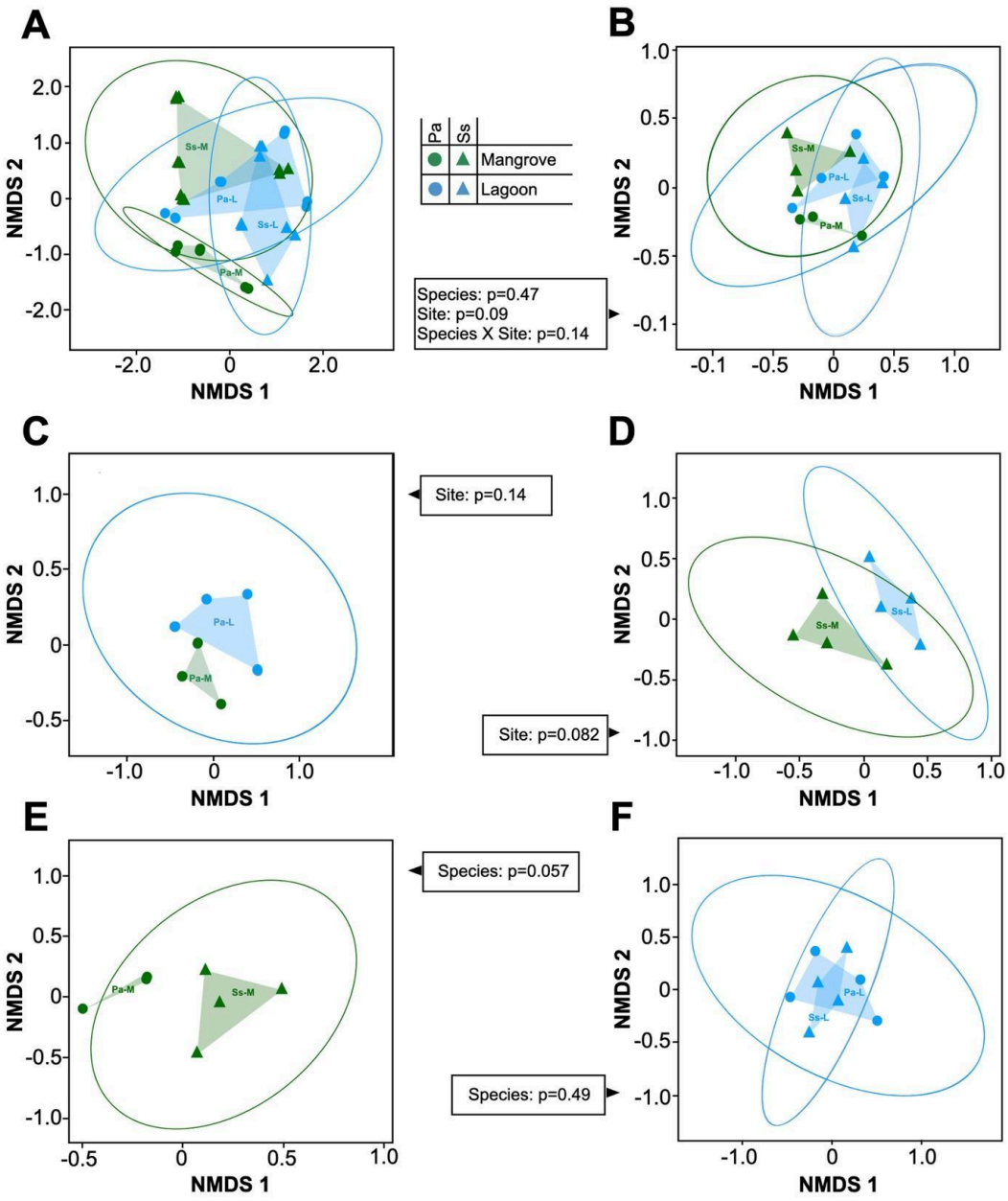

Figure 2.9. Non-metric dimensional scaling (NMDS) analysis based on Bray Curtis distances between samples calculated from abundance of bacterial ASVs. **(A)** All samples, including replicate samples from the same coral. **(B)** All corals, with replicates averaged. **(C)** *P. astreoides* only. **(D)** *S. siderea* only. **(E)** Mangrove corals only. **(F)** Lagoon corals only. Ellipses represent 95% confidence intervals for the distribution of samples in each coral-by-site combination. In panels B-F, p-values resulting from the PERMANOVA analyses are shown.

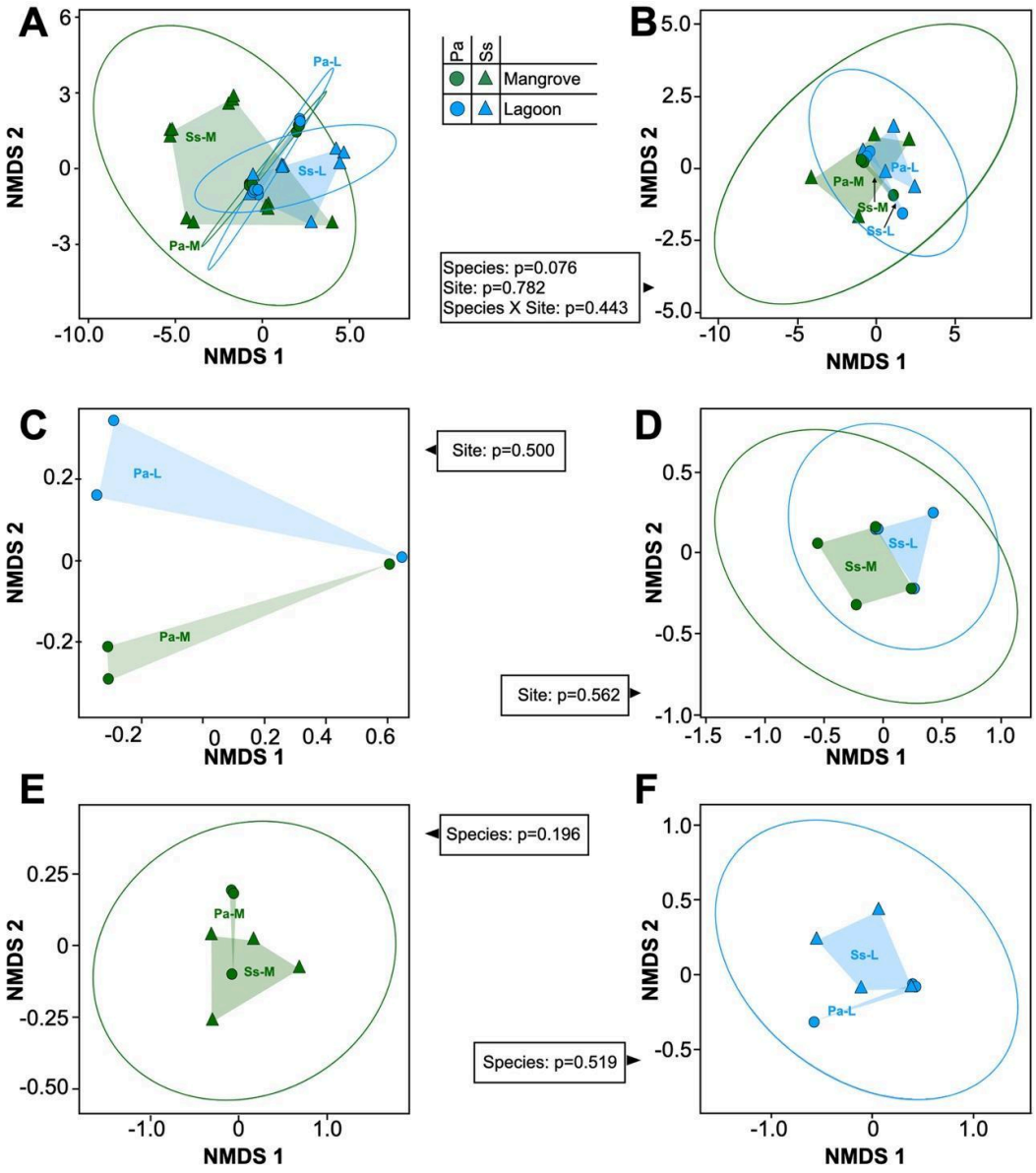

Figure 2.10. Non-metric dimensional scaling (NMDS) analysis based on Bray Curtis distances between samples calculated from abundance of archaeal ASVs. **(A)** All samples, including replicate samples from the same coral. **(B)** All corals, with replicates averaged. **(C)** *P. astreoides* only. **(D)** *S. siderea* only. **(E)** Mangrove corals only. **(F)** Lagoon corals only. Ellipses represent 95% confidence intervals for the distribution of samples in each coral-by-site combination. In panels B-F, p-values resulting from the PERMANOVA analyses are shown.

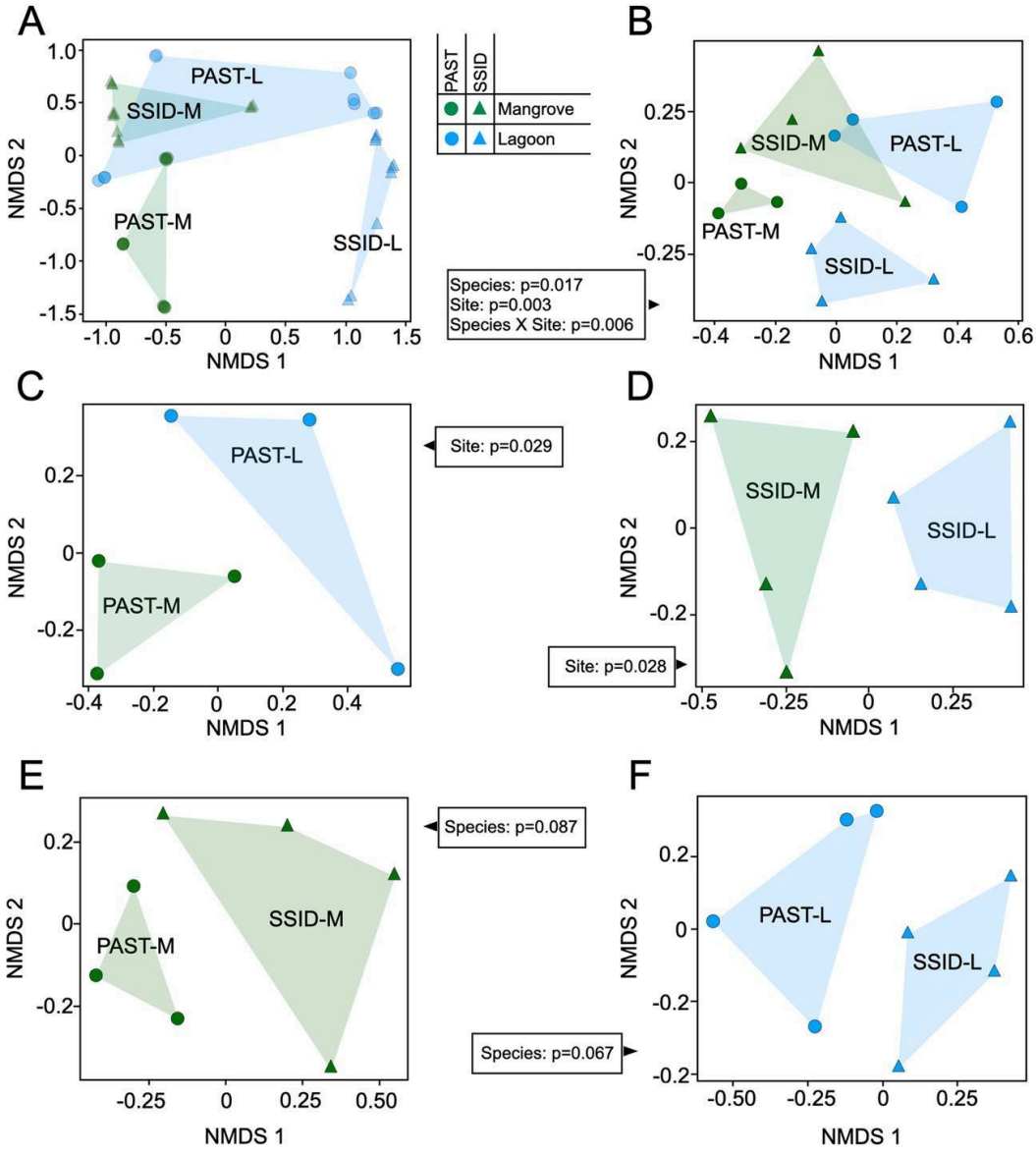

Figure 2.11. Non-metric dimensional scaling (NMDS) analysis based on Bray Curtis distances between samples calculated from abundance of chloroplast ASVs. **(A)** All samples, including replicate samples from the same coral. **(B)** All corals, with replicates averaged. **(C)** *P. astreoides* only. **(D)** *S. siderea* only. **(E)** Mangrove corals only. **(F)** Lagoon corals only. Ellipses represent 95% confidence intervals for the distribution of samples in each coral-by-site combination. In panels B-F, p-values resulting from the PERMANOVA analyses are shown.

The NMDS analyses of chloroplast ASVs did reveal significant differences between samples based on species, site, and the combination of species by site (Fig. 2-11).

Indicator species identification

To determine if specific taxa are statistically overrepresented in particular species-by-site combinations, I conducted indicator species analyses for Archaea and chloroplasts. The archaeal analysis identified one significant indicator for *P. astreoides* in the mangrove habitat and one significant indicator for *S. siderea* in the lagoon (Fig. 2-12A). In both cases, the top hits in the NCBI nr database with taxonomic annotation below the level of Archaea correspond to the Phylum Nitrososphaerota (formerly Thaumarchaeota). An alignment of the two sequences reveals that they differ at 11 of 250 nucleotide positions (Fig. 2-12B).

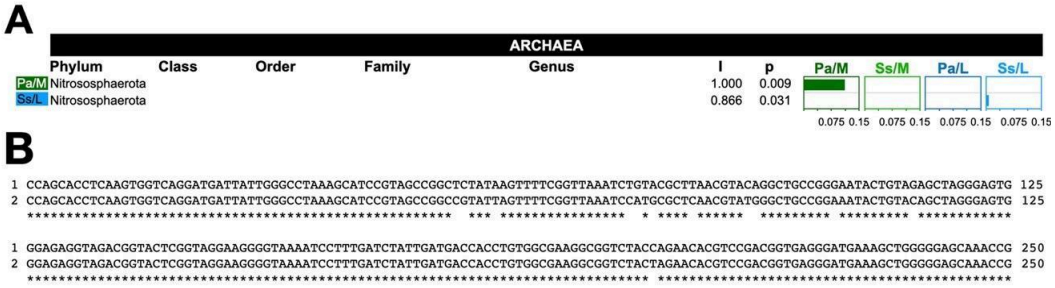

Figure 2.12. (A) Significant indicator species among Archaea ASVs. The relative abundance of each indicator species in each of the four species-by-habitat combinations is shown in the panels to the right: (Pa=*Porites astreoides*; Ss=*Siderastrea siderea*; M=mangrove; L=lagoon; I=indicator statistic, which ranges from 0 to 1; p=p-value of indicator statistic). Only ASVs with I>0.8 and p≤0.05 are shown. **(B)** An alignment of 16S sequences is provided for the two significant archaean indicator species identified.

Eleven significant indicator species were identified among the chloroplast ASVs: six for *P. astreoides* in mangrove, three for *P. astreoides* in lagoon, one for *S. siderea* in mangrove, and one for *S. siderea* in lagoon (Fig. 2.12) (Figure 2.8). Based on *BLASTn* searches of the NCBI non-redundant nucleotide databases, we identified the top-match to each sequence for which there was taxonomic annotation below the level of chloroplasts. Two of these indicators exhibited affinity to Foraminifera, four exhibited affinity to *Ostreobium*, and two exhibited affinity to Apicomplexa. The two Foraminifera indicator sequences, both indicators of *P. astreoides* in the mangrove, differed at five nucleotides. The four *Ostreobioum* sequences, which were indicators or *P. astreoides* in the mangrove (2) or lagoon (1) and *S. siderea* in the lagoon differed at 17 positions, with individual sequences differing by 4-11 nucleotides. The two Apicomplexa sequences, both indicators of *P. astreoides* in the lagoon, differed at only 1 nucleotide.

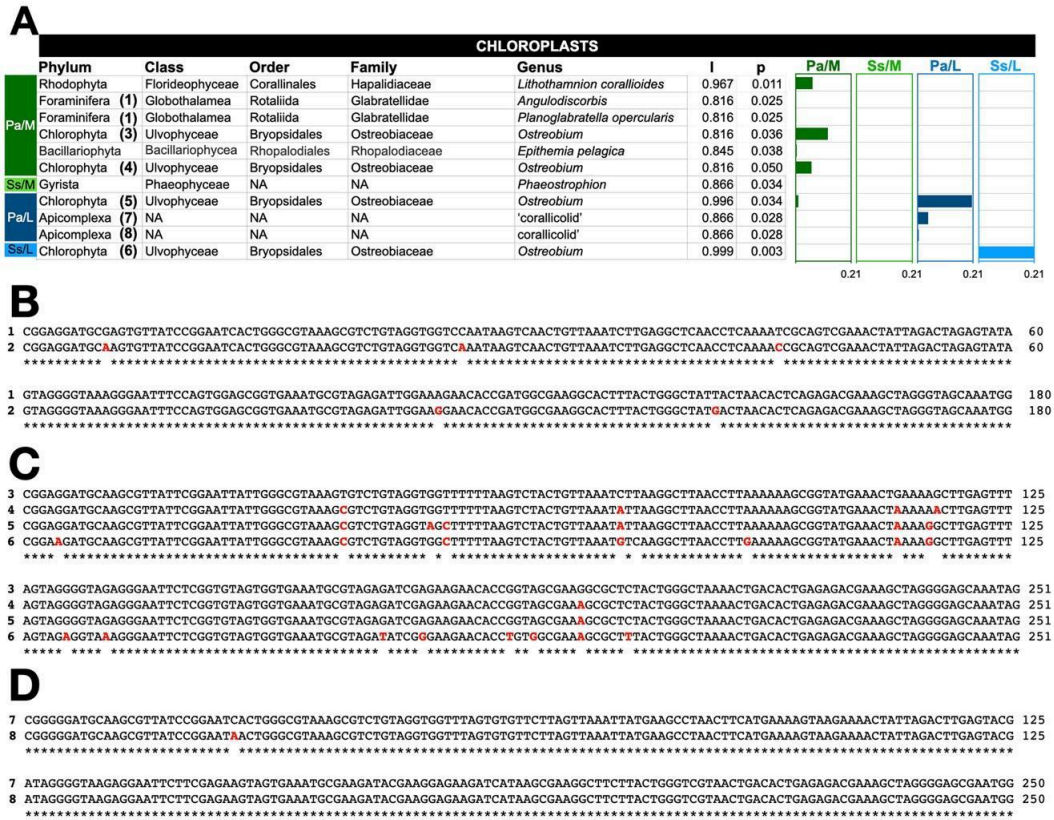

Figure 2.13. (A) Significant indicator species among Chloroplast ASVs. The relative abundance of each indicator species in each of the four species-by-habitat combinations is shown in the panels to the right: (Pa=*Porites astreoides*; Ss=*Siderastrea siderea*; M=mangrove; L=lagoon; I=indicator statistic, which ranges from 0 to 1; p=p-value of indicator statistic). Only ASVs with I>0.8 and p≤0.05 are shown. **(B)** An alignment of 16S sequences from the two Foraminifera-related indicator species (1-2). **(C)** An alignment of 16S sequences from the four *Ostreobium*-related indicator species (3-6). **(D)** An alignment of 16S sequences from the two Apicomplexa-related indicator species (7-8). Differences relative to the top sequence are shown in bold, red type in each alignment.

Discussion

As the future survival of corals is under threat from climate change and associated anthropogenic stressors, there is growing interest in the role that the

microbiome might play in coal stress resistance. Microbes associated with corals have been found to reduce bleaching impacts and reduce thermal and pathogen stresses on their coral hosts (Rosado et al. 2019). Recently, targeted manipulation of the coral microbiome via “probiotics” has been proposed as a treatment to increase coral pathogen defense and bleaching resistance, and accelerate recovery from bleaching (Welsh et al. 2017; Rosado et al. 2019). Beneficial microorganisms for corals (BMCs) have been found to improve coral nutrient cycling and overall health; however, exactly how BMCs benefit corals is not generally well understood (Welsh et al. 2017; Rosado et al. 2019).

In this chapter, I described my contribution to a collaborative study on the microbiome of mangrove and lagoon corals. The study is based on amplifying a fragment of 16S ribosomal DNA using primers that are targeted primarily for Bacteria (Apprill et al. 2015; Parada et al. 2016). Such surveys typically recover many archaeal 16S sequences as well as 16S sequences from chloroplasts and mitochondria, eukaryotic organelles that are derived from bacteria. However, these archaeal and organelle sequences are commonly treated as contamination and removed from further analysis. The present study demonstrates the value of analyzing archaeal sequences as well as chloroplast sequences, including the value of them in 16S metabarcoding studies that do not explicitly targeting these taxa. Even after removing the low-abundance ASVs, and those unique to a single sample, we still recovered over 600 distinct archaeal sequences, or about 60% of

the number of bacterial sequences we recovered (Fig. 2.5). Furthermore, the average abundance of individual archaeal ASVs within each sample was comparable to the abundance of individual bacterial ASVs, although there were, on average, about 10 times as many distinct bacterial ASVs recovered per sample. We recovered fewer chloroplast ASVs, but the average abundance of each distinct chloroplast ASV was much higher than either the bacterial or archaeal ASVs. Among the chloroplasts we identified were a phylogenetically wide range of known coral symbionts, including the microscopic endolithic gree alga, *Ostreobium*, and the apicomplexan coral associate, *Corallicoles*.

This is the first metagenomic study to compare corals living as mangrove epibionts to conspecifics living in a sunny benthic habitat. A previous study by Camp and co-workers compared three species of Pacific corals in a mangrove-lined lagoon versus shallow reef habitats (Camp et al. 2020). The "mangrove" corals in the Camp et al. study are comparable to the "lagoon" corals in this study. By contrast, the mangrove corals in this study were shaded by the overlying mangrove canopy, with most growing suspended on the prop roots of red mangrove. Given this qualitative difference in the degree of shading, the mangrove corals in the present study would presumably be less able than the lagoon corals to rely on autotrophy from their photosynthetic symbionts, and more reliant on heterotrophy through a combination of predation or the absorption

of dissolved nutrients. This kind of trophic difference could drive changes in the microbiome related to metabolism and nutrient cycling.

Given the difference in habitat and species, we were particularly interested in discovering whether particular indicator species might be over-represented in each of the four species-by-habitat combinations. Among the 602 Archaean ASVs we analyzed, only two appeared to be significant indicator species, both from the phylum Nitrososphaerota. We currently know very little about the function of Archaea within coral microbiomes and whether they might aid in nutrient cycling. It has been suggested that ammonia-oxidizing Nitrososphaerota could contribute to nitrogen cycling in corals (Mohamed et al. 2023). A previous study assembled two distinct Nitrososphaerota genomes from the *Porites lutea* genome, including enzymatic pathways that could aid the coral's symbiosis with Symbiodiniaceae (Robbins et al. 2019).

Eukaryotic chloroplasts

This study identified 11 different 'indicator species' among the chloroplast ASVs that were significantly enriched in one of the species/habitat combinations. Among these eleven sequences, blast similarity suggested the presence of multiple hits from three taxa, all of which are known to form symbiosis with scleractinian corals: the green alga Ostreobium, Foraminifera, and Apicomplexa.

Ostreobium sp. **(Chlorophyta)**

Ostreobium is a microscopic, endolithic green alga which, when present in abundance, creates a green band in the coral skeleton beneath the live tissue (del Campo et al. 2016; Verbruggen et al. 2017). *Ostreobium* benefits corals by supplying photosynthates and by shielding coral hosts from stress caused by excess light (del Campo et al. 2016; Verbruggen et al. 2017). However, they can rapidly degrade the skeletons of both live and dead corals through carbonate dissolution (Aline 2008). *Ostreobium quekettii* has been shown to be widely distributed across coral species (over 85%) and was found adaptable to low light (Gutner-Hoch and Fine 2011). This species was also hypothesized to provide photosynthates and nutrients to corals as an alternative to zooxanthellae during bleaching events (Fine and Loya 2002).

Apicomplexans

Two nearly identical apicomplexan chloroplast sequences were identified as indicator species in the *P. astreoides* lagoon samples (Fig 2.13). Apicomplexans are well known as obligate intracelluar parasites responsible for human diseases, including malaria and toxoplasmosis (Seeber and Steinfelder 2016). These organisms evolved when a single-celled eukaryotic ancestor acquired a photosynthetic eukaryote as an intracellular symbiont. The parasites which evolved from this photosynthetic ancestor subsequently lost photosynthetic ability and ability to synthesize chlorophyll. Recently, apicomplexan 'corallicoids' were found to be the second most abundant microscopic eukaryotic

associate of corals after only zooxanthellae (Kwong et al. 2019). Unlike parasitic apicomplexans, the corallicoids retain four chlorophyll photosynthesis genes, but they lack the enzymes for a functional photosystem. The function of chlorophyll in these organisms and their contribution to the coral microbiome are not yet known (del Campo et al. 2016).

Conclusion

In conclusion, corals host many possible symbionts including diverse bacteria, archaea, eukaryotes and viruses. We documented some significant differences between mangrove and lagoonal representatives of the same coral species, and between coral species occupying the same habitat. Much more data are required to understand the functional implications of such differences in the composition of the coral holobiont across species and habitats.

BIBLIOGRAPHY

Aichelman HE, Bove CB, Castillo KD, Boulton JM, Knowlton AC, Nieves OC, Ries JB, Davies SW (2021) Exposure duration modulates the response of Caribbean corals to global change stressors. *Limnology and Oceanography* 66:3100–3115.

Aline T (2008) Dissolution of dead corals by euendolithic microorganisms across the northern Great Barrier Reef (Australia). *Microbial Ecology* 55:569–580.

Alvarez-Yela AC, Mosquera-Rendón J, Noreña-P A, Cristancho M, López-Alvarez D (2019) Microbial diversity exploration of marine hosts at Serrana Bank, a coral atoll of the Seaflower Biosphere Reserve. *Frontiers in Marine Science* 6:338. doi: 10.3389/fmars.2019.00338

Apprill A, McNally S, Parsons R, Weber L (2015) Minor revision to V4 region SSU rRNA 806R gene primer greatly increases detection of SAR11 bacterioplankton. *Aquatic Microbial Ecology* 75:129–137.

Baker AC (2003) Flexibility and specificity in coral-algal symbiosis. *Annual Review of Ecology, Evolution, and Systematics* 34:661–689.

Beltran-Torres AU, Carricart-Gavinet JP (1993) Skeletal morphologic variation in Montastrea cavernosa (Cnidaria: Scleractinia) at Isla Verde Coral Reef, Veracruz, Mexico. *Revista de Biología Tropical* 41:559–562.

Bengtsson ZA, Kuhn KM, Battaglino AT, Li AS, Talbot MN, Wafapoor M, Atta CJ, Kowalski MB, Margolis SP, Rar EA, Burmester EM, Lesneski KC, Scavo K, Kaufman L, Stewart NL, Finnerty JR (2019) Corals of the genus Porites are a locally abundant component of the epibiont community on mangrove prop roots at Calabash Caye, Turneffe Atoll, Belize. *Caribbean Naturalist* 2019(67). https://hdl.handle.net/2144/40611

Bonthond G, Merselis DG, Dougan KE, Graff T, Todd W, Fourqurean JW, Rodriguez-Lanetty M (2018) Inter-domain microbial diversity within the coral holobiont Siderastrea siderea from two depth habitats. *PeerJ* 6:e4323. https://doi.org/10.7717/peerj.4323

Bove CB, Ries JB, Davies SW, Westfield IT, Umbanhowar J, Castillo KD (2019) Common Caribbean corals exhibit highly variable responses to future acidification and warming. *Proceedings. Biological Sciences* 286(1900):20182840. https://doi.org/10.1098/rspb.2018.2840

Callahan BJ, McMurdie PJ, Rosen MJ, Han AW, Johnson AJ, Holmes SP (2016) DADA2: High-resolution sample inference from Illumina amplicon data. *Nature Methods* 13:581–583.

Camp EF, Suggett DJ, Gendron G, Jompa J, Manfrino C, Smith DJ (2016) Mangrove and seagrass beds provide different biogeochemical services for corals threatened by climate change. *Frontiers in Marine Science* 3:52. doi: 10.3389/fmars.2016.00052

Camp EF, Sugget DJ, Pogoreutz C, Nitschke MR, Houlbreque F, Hume BCC, Gardner SG, Zampighi M, Rodolfo-Metalpa R, Voolstra CR (2020) Corals exhibit distinct patterns of microbial reorganisation to thrive in an extreme inshore environment. *Coral Reefs* 39:709–716

Castillo KD, Helmuth B (2003) Effects of elevated seawater temperature on photosynthesis and respiration in scelractinian coral Montastraea annularis - Southern Belize. *Integrative and Comparative Biology* 43(6):819. https://sicb.org/abstracts/effects-of-elevated-seawater-temperature-on-photosynthesis-and-respiration-in-scelractinian-coral-montastraea-annularis-southern-belize/

De Cáceres M, Legendre P (2009) Associations between species and groups of sites: indices and statistical inference. *Ecology* 90:3566–3574.

De Cáceres M, Legendre P, Moretti M (2010) Improving indicator species analysis by combining groups of sites. *Oikos* 119:1674–1684.

del Campo J, Pombert JF, Slapeta J, Larkum A, Keeling PJ (2016) The 'other' coral symbiont: Ostreobium diversity and distribution. *ISME Journal* 11:296–299.

Fine M, Loya Y (2002) Endolithic algae: an alternative source of photoassimilates during coral bleaching. *Proceedings. Biological Sciences* 269(1497):1205–1210. https://doi.org/10.1098/rspb.2002.1983

Gutner-Hoch E, Fine M (2011) Genotypic diversity and distribution of Ostreobium quekettii within scleractinian corals. *Coral Reefs* 30:643–650.

Hernández Fernández L (2015) Stony corals on submerged mangrove roots of Rhizophora mangle L. in Jardines de la Reina National Park, Cuba. *Revista Investigaciones Marinas* 35:16–20.

Hoegh-Guldberg O, Mumby PJ, Hooten AJ, Steneck RS, Greenfield P, Gomez E, Harvell CD, Sale PF, Edwards AJ, Caldeira K, Knowlton N, Eakin CM, Iglesias-Prieto R, Muthiga N, Bradbury RH, Dubi A, Hatziolos ME (2007) Coral reefs under rapid climate change and ocean acidification. *Science* 318(5857):1737–1742. https://doi.org/10.1126/science.1152509

Howard RD, Schul MD, Bravo LMR, Altieri AH, Meyer JL (2023) Shifts in the coral microbiome in response to *in situ* experimental deoxygenation. *Applied and Environmental Microbiology* 89(11). https://doi.org/10.1128/aem.00577-23

Hughes TP, Baird AH, Bellwood DR, Card M, Connolly SR, Folke C, Grosberg R, Hoegh-Guldberg O, Jackson JBC, Kleypas J, Lough JM, Marshall P, Nystrom M, Palumbi SR, Pandolfi JM, Rosen B, Roughgarden J (2003) Climate change, human impacts, and the resilience of coral reefs. *Science* 301(5635):929–933. https://doi.org/10.1126/science.1085046

Ju H, Zhang J, Zou Y, Xie F, Tang X, Zhang S, Li J (2024) Bacteria undergo significant shifts while archaea maintain stability in Pocillopora damicornis under sustained heat stress. *Environmental Research* 250:118469. https://doi.org/10.1016/j.envres.2024.118469

Knowlton N, Rohwer F (2003) Multispecies microbial mutualisms on coral reefs: The host as a habitat. *American Naturalist* 162:S51–S62

Kwong WK, Del Campo J, Mathur V, Vermeij MJA, Keeling PJ (2019) A widespread coral-infecting apicomplexan with chlorophyll biosynthesis genes. *Nature* 568(7750): 103–107. https://doi.org/10.1038/s41586-019-1072-z

Lahti L, Shetty S (2017) Tools for microbiome analysis in R LaJeunesse TC, Parkinson JE, Gabrielson PW, Jeong HJ, Reimer JD, Voolstra CR, Santos SR (2018) Systematic revision of Symbiodiniaceae highlights the antiquity and diversity of coral endosymbionts. *Current Biology* 28:2570–2580 e2576.

McDevitt-Irwin JM, Baum JK, Garren M, Thurber RLV (2017) Responses of Coral-Associated Bacterial Communities to Local and Global Stressors. *Frontiers in Marine Science* 4:262. doi: 10.3389/fmars.2017.00262

Meyer JL, Paul VJ, Teplitski M (2014) Community shifts in the surface microbiomes of the coral Porites astreoides with unusual lesions. *PLoS One* 9(6):e100316. https://doi.org/10.1371/journal.pone.0100316

Mohamed AR, Ochsenkuhn MA, Kazlak AM, Moustafa A, Amin SA (2023) The coral microbiome: towards an understanding of the molecular mechanisms of coral-microbiota interactions. *FEMS Microbiology Reviews* 47(2):fuad005. https://doi.org/10.1093/femsre/fuad005

Munday PL, Warner RR, Monro K, Pandolfi JM, Marshall DJ (2013) Predicting evolutionary responses to climate change in the sea. *Ecology Letters* 16(12):1488–1500. https://doi.org/10.1111/ele.12185

Oliver TA, Palumbi SR (2011) Do fluctuating temperature environments elevate coral thermal tolerance? *Coral Reefs* 30:429–440.

Olson ND, Ainsworth TD, Gates RD, Takabayashi M (2009) Diazotrophic bacteria associated with Hawaiian montipora corals: Diversity and abundance in correlation with symbiotic dinoflagellates. *Journal of Experimental Marine Biology and Ecology* 371:140–146.

Palumbi SR, Barshis DJ, Traylor-Knowles N, Bay RA (2014) Mechanisms of reef coral resistance to future climate change. *Science* 344(6186):895–898. https://doi.org/10.1126/science.1251336

Parada AE, Needham DM, Fuhrman JA (2016) Every base matters: assessing small subunit rRNA primers for marine microbiomes with mock communities, time series and global field samples. *Environmental Microbiology* 18(5):1403–1414. https://doi.org/10.1111/1462-2920.13023

Robbins SJ, Singleton CM, Chan CX, Messer LF, Geers AU, Ying H, Baker A, Bell SC, Morrow KM, Ragan MA, Miller DJ, Foret S, ReFuGe C, Voolstra CR, Tyson GW, Bourne DG (2019) A genomic view of the reef-building coral Porites lutea and its microbial symbionts. *Nature Microbiology* 4:2090–2100.

Rodriguez-Lanetty M, Granados-Cifuentes C, Barberan A, Bellantuono AJ, Bastidas C (2013) Ecological Inferences from a deep screening of the Complex Bacterial Consortia associated with the coral. *Molecular Ecology* 22(16):4349–4362. https://doi.org/10.1111/mec.12392

Rogers CS (2017) A unique coral community in the mangroves of Hurricane Hole, St. John, US Virgin Islands. *Diversity* 9(3):29. https://doi.org/10.3390/d9030029

Rogers CS, Herlan JJ (2012) Life on the edge: corals in mangroves and climate change *Proceedings of the 12th International Coral Reef Symposium, Cairns, Australia*. https://www.icrs2012.com/proceedings/manuscripts/ICRS2012_9A_13.pdf

Rosado PM, Leite DCA, Duarte GAS, Chaloub RM, Jospin G, Nunes da Rocha U, J PS, Dini-Andreote F, Eisen JA, Bourne DG, Peixoto RS (2019) Marine probiotics: increasing coral resistance to bleaching through microbiome manipulation. *ISME Journal* 13:921–936

Scavo Lord K, Barcala A, Aichelman HE, Kriefall NG, Brown C, Knasin L, Secor R, Tone C, Tsang L, Finnerty JR (2021) Distinct phenotypes associated with mangrove and lagoon habitats in two widespread Caribbean corals, Porites astreoides and Porites divaricata. *Biological Bulletin* 240(3):169–190. https://doi.org/10.1086/714047

Scavo Lord K, Lesneski KC, Bengtsson ZA, Kuhn KM, Madin J, Cheung B, Ewa R, Taylor J, Burmester EM, Morey J, Kaufman L, Finnerty JR (2020) Multi-year viability of a reef coral population living on mangrove roots suggests an important role for

mangroves in the broader habitat mosaic of corals. *Frontiers in Marine Science* 7:377. doi: 10.3389/fmars.2020.00377

Seeber F, Steinfelder S (2016) Recent advances in understanding apicomplexan parasites. *F1000Research* 5:F1000 Faculty Rev-1369. https://doi.org/10.12688/f1000research.7924.1

Speare L, Davies SW, Balmonte JP, Baumann J, Castillo KD (2020) Patterns of environmental variability influence coral-associated bacterial and algal communities on the Mesoamerican Barrier Reef. *Molecular Ecology* 29:2334–2348

Studivan MS, Milstein G, Voss JD (2019) Montastraea cavernosa corallite structure demonstrates distinct morphotypes across shallow and mesophotic depth zones in the Gulf of Mexico. *PLoS One* 14:e0203732

van Oppen MJH, Blackall LL (2019) Coral microbiome dynamics, functions and design in a changing world. *Nature Reviews. Microbiology* 17(9):557–567. https://doi.org/10.1038/s41579-019-0223-4

Verbruggen H, Marcelino VR, Guiry MD, Cremen MCM, Jackson CJ (2017) Phylogenetic position of the coral symbiont Ostreobium (Ulvophyceae) inferred from chloroplast genome data. *Journal of Phycology* 53(4):790–803. https://doi.org/10.1111/jpy.12540

Veron JEN (2000) *Corals of the World*. Townsville MC, Qld, Australia: Australian Institute of Marine Science and CRR Ald Pty Ltd.

Wang L, Shantz AA, Payet JP, Sharpton TJ, Foster A, Burkepile DE, Thurber RV (2018) Corals and their microbiomes are differentially affected by exposure to elevated nutrients and a natural thermal anomaly. *Frontiers in Marine Science* 5:101. doi: 10.3389/fmars.2018.00101

Wegley L, Edwards R, Rodriguez-Brito B, Liu H, Rohwer F (2007) Metagenomic analysis of the microbial community associated with the coral Porites astreoides. *Environmental Microbiology* 9(11):2707–2719. https://doi.org/10.1111/j.1462-2920.2007.01383.x

Welsh RM, Rosales SM, Zaneveld JR, Payet JP, McMinds R, Hubbs SL, Vega Thurber RL (2017) Alien vs. predator: bacterial challenge alters coral microbiomes unless controlled by Halobacteriovorax predators. *PeerJ* 5:e3315.

Yates KK, Rogers CS, Herlan JJ, Brooks GR, Smiley NA, Larson RA (2014) Diverse coral communities in mangrove habitats suggest a novel refuge from climate change. *Biogeosciences* 11:4321–4337.

Ziegler M, Grupstra CGB, Barreto MM, Eaton M, BaOmar J, Zubier K, Al-Sofyani A, Turki AJ, Ormond R, Voolstra CR (2019) Coral bacterial community structure responds to environmental change in a host-specific manner. *Nature Communications* 10(1):3092. https://doi.org/10.1038/s41467-019-10969-5

Vita